

Control of liquid optically clear adhesive overflow in Optical Bonding process

José Pedro Moreira da Silva Teles

MSc THESIS

Supervisor in Bosch: Eng. Miguel Nogueira

Supervisor in FEUP: Prof. José Marafona



Master Integrated in Mechanical Engineering

(July 2018)

“When something is important enough, you do it even if the odds are not in your favour”

Elon Musk

Abstract

The automotive industry is developing the Car Multimedia (CM) sector for the past decades. Along with the growth of this branch, a wide range of new CM products appeared in the automotive industry, especially in the last years with the appearance of display devices such as LCD (Liquid Crystal Display) and LED (Light Emitting Diode) in these products. To tackle the need of enhancing the optical properties of these devices, being that this application requires that the display is readable in a bright ambient conditions, the Optical Bonding process started being used in these products. The quality of display with Optical Bonding is undoubtedly greater for it significantly reduces reflections. Nevertheless it may be challenging for the process engineers to keep the process stable when a new product with a different concept and components is being introduced in the production line.

This work aims to study the process and seek a possible solution to reduce the number of rejections in the Optical Bonding process for a new IS (Instrumentation System) product. The rejection is caused by the overflow of LOCA (Liquid Optically Clear Adhesive) out of the active area of the display, causing intrusion of this substance in the interior of the display. After the early study about the process and the phenomena associated, it was suggested to execute two DOE (Design Of Experiment) in order to find a solution. One of them consists on assessing if a surface deactivation plasma treatment in the outer frame of the display is capable of causing dewetting effect on the LOCA that is overflowing from the active area. The evaluation of this effect is done by measuring the surface energy of the material coating the surface which is one of the factors, and then dispense one drop of LOCA in the middle of the coating lines, further apply a vertical force and observe if there is dewetting effect when LOCA reaches the zones coated zones. The measurement of Surface energy is an input for a surface deactivation plasma treatment that may be designed if this experiment brings satisfactory results. This DOE is presented in this dissertation although it is not yet performed. The other DOE focus on assessing if it is possible to cure LOCA where this problem happens right after assembly. For this matter it was designed and built an experimental setup including a prototype system with the function of blowing hot air into these areas. The goal is to evaluate if it is able to contain the problem before the adhesive reaches the tape or there is intrusion, through triggering an earlier cure of the material in this zones. The factors tested in the DOE are time of this additional step in the process and temperature of the air stream in contact with the product. It was possible to conclude that the use of a pre-cure system can effectively stop LOCA overflow from causing intrusions of this substance in the interior of

the display if both factors are set to the maximum level tested. Furthermore, it was designed a new system that is able to perform this effect without increasing the cycle time of the Optical Bonding process studied.

Resumo

A indústria automotiva está a desenvolver o sector de Car Multimedia (CM) nas ultimas décadas. Ao longo do crescimento deste ramo, uma vasta gama de novos produtos de CM apareceram na indústria automotiva, especialmente com o aparecimento de displays nestes produtos, como os LCD e os LED. Para responder à necessidade de melhorar as propriedades ópticas destes dispositivos, já que esta aplicação requiere que o display seja legível em condições ambientais com elevada luminosidade, o Optical Bonding começou a ser usado nestes produtos. A melhoria de qualidade ao usar Optical Bonding nestes dispositivos é indiscutível já que reduz a reflexão de forma significativa. Por outro lado, é um desafio para os engenheiros de processo manter o processo estável quando um novo produto com diferente conceito e componentes é introduzido na linha de produção.

Este trabalho visa o estudo do processo com vista a encontrar uma solução para reduzir o numero de rejeições na linha de Optical Bonding para um novo produto de sistema de instrumentação (IS). Este problema de rejeição é em grande parte devido ao adesivo liquido opticamente transparente (LOCA) que transborda da zona ativa do display, causando a intrusão desta substância no interior do display. Depois de um estudo prévio sobre o processo e os fenómenos associados, foi proposta a execução de dois Design Of Experiment (DOE) com o objetivo de encontrar uma solução. Um deles consiste em avaliar se um material de baixa energia superficial aplicado na *frame* exterior do display é capaz de causar o efeito de *dewetting* na LOCA que está a transbordar da área ativa do display. A avaliação deste efeito é realizada através de medições energia superficial no revestimento da superfície que é um dos fatores, ao que se segue dispensação de uma gota de LOCA no meio de duas linhas do revestimento de superfície, posteriormente aplicar uma força vertical na LOCA e verificar se há efeito de *dewetting* quando a LOCA se espalha e entra em contacto com o material de baixa energia superficial. A medição de energia superficial é um parâmetro de entrada para projetar um tratamento de plasma de desativação de superfície que possa ser concebido para esta aplicação caso haja resultados satisfatórios. Este DOE é apresentado nesta dissertação apesar de ainda não ter sido executado. O outro DOE foca-se em averiguar se é possível curar a LOCA nas áreas onde este problema acontece imediatamente após montagem. Para isto foi projetado e construído um setup experimental que inclui um sistema protótipo com a função de fornecer ar quente nas áreas do display afetadas por este problema. O objetivo é avaliar se o sistema é capaz de conter o problema antes do adesivo chegar à fita de isolamento ou haja intrusão do mesmo no *display*, através do começo a cura do material nestas zonas mais cedo.

Os factores testados neste DOE são o tempo deste passo adicional no processo e a temperatura do ar que está em contacto com o produto. Foi possível concluir que o uso de um sistema de pré-cura consegue que a LOCA não transborde da zona ativa do *display*, causando intrusões no interior do mesmo, para o nível máximo de ambos os factores testados. Posteriormente, foi desenhado um novo sistema que consegue executar este passo adicional no processo sem aumentar o tempo de ciclo do processo de Optical Bonding estudado neste trabalho.

Acknowledgment

Firstly, thanks to Bosch Car Multimedia for the opportunity to develop this project in the context of the master thesis. Special thanks to the COC of Optical Bonding process Miguel Nogueira, for his dedication, patience, motivation, for all the expertise shared about Optical Bonding, for all the guidance and support during the phases of prototype development and experimental work, and also for all the resources and facilities provided. Thanks to the director of MFE-MTN Xavier Faria who gave me full support to develop the project and for the many lessons learned. Also, I need to express my gratitude to the Director of MFE-SEI José Brito, my mentor during the first four months of the internship, who played an essential role in my professional growth, who taught me so much about industrial processes, data monitoring, troubleshooting and teamwork. Another word of appreciation to Miguel Rosmaninho for the experience and the knowledge shared. Nevertheless, thanks to every co-worker from the many departments of Bosch Car Multimedia that somehow collaborated in the project, their assistance was indispensable to its completion.

A special word of gratitude to Professor José Marafona that always supported me along the whole internship and project and that reviewed this dissertation, for all his advice, readiness, sympathy and trust.

Thanks to all the partners from FEUP involved. Namely, the director of MIEM and ADFEUP Lucas da Silva and ADFEUP engineers Ricardo Carbas and Eduardo Marques for the consulting support provided in the design of the low surface energy treatment experiment. Also, a word of gratitude to the persons that supported the previous project of my internship, namely professor Alexandre Lopes for all the guidance and help CFD analysis and professor Madalena Dias for giving me access to Ansys research license, who allowed me to learn so much about fluid flows analysis even if the results were inconclusive. Thanks to professor Alexandre Afonso for giving the motivation, sympathy and creativity in the brainstorm session during the early phases of the project.

Thanks to 3Dadd for the consulting support and perfect execution of custom parts using additive manufacturing.

Thanks to Luis Santos from Lizmontagens Thermal Technologies for the cooperation and effectiveness in responding to the needs of the project

A final word of appreciation to Vitória, my family and my friends. They were my angular stone during these project, and for that I will be forever grateful.

At last, thanks to Bosch Car Multimedia for paying my internship and giving financial support to the project. Without it none of the experimental work would be possible.

Contents

1. INTRODUCTION.....	9
1.1 Project background and motivation.....	9
1.2 The project at Bosch Car Multimedia.....	10
1.3 Methodology and structure of dissertation.....	11
1.4 Project goals.....	13
2. STATE OF THE ART.....	15
2.1 Optical Bonding.....	15
2.2 LOCA.....	19
2.3 Wetting and spreading.....	22
2.4 Factorial DOE.....	26
3. DESIGN OF EXPERIMENT.....	29
3.1 Overflow cure system.....	29
3.2 Concept low surface energy treatment.....	37
4. EXPERIMENTAL SETUP.....	44
4.1 Concept system to cure overflow.....	44
4.2 Overflow Cure System.....	45
4.3 Components selection and Benchmarking.....	46
4.4 Assembly and setup.....	49
4.4.1 OCS version 1.....	49
4.4.2 OCS version 2.....	52
4.5 Supports for product during experiment.....	60
5. EXPERIMENTAL DATA ANALYSIS.....	66
5.1 Results description and DOE analysis.....	66
5.2 Implementation.....	76
6. CONCLUSIONS AND FUTURE WORK.....	78
REFERENCES.....	80
A. ATTACHMENT of Technical sheets.....	83
B. ATTACHMENT of Technical Drawings of OCS.....	93

List of acronyms

BPS	Bosch Production System
DOE	Design Of Experiment
DSC	Differential Scanning Calorimetry
ESD	Electro Static Discharge
FDM	Fused Deposition Modeling
FRL	Filter Regulator Lubricator
IS	Instrumentation System
LOCA	Liquid Optically Clear Adhesive
MSA	Mobile Surface Analysis
OCS	Overflow Cure System
LCD	Liquid Crystal Display
OCA	Optically Clear Adhesive
OEE	Overall Equipment Efficiency
PID	Proportional Integral Derivative controller
PSA	Pressure Sensitive Adhesive
RP	Rapid Prototyping

Notation

γ_{lv}	Surface tension of liquid
γ_{sv}	Surface free energy of a solid
γ_{sl}	Surface tension between solid and liquid
θ	Contact angle
θ_{eq}	Contact angle in equilibrium state
S_{eq}	Equilibrium Spreading Coefficient

List of Figures

Figure 1 – IS product for motorcycles produced by Bosch CM	9
Figure 2 – Infiltration of LOCA in the interior of the display	10
Figure 3 – Methodology diagram	11
Figure 4 – Schematic comparison of Optical Bonding and air gap in terms of: light loss (left) and glare (right) [4].....	16
Figure 5 – Example of clean room (ValuLine Hardwall Modular Cleanroom)	17
Figure 6 - – Scheme of Direct Dry Film Optical Bonding [7].....	18
Figure 8 - Cure time of silicon A as a function of cure temperature for different heat rates ...	21
Figure 9 – Evolution of viscosity of the material with time for different cure temperatures ...	22
Figure 10 – Representation of acting forces on the contact line between a solid and a liquid layer [1].....	23
Figure 11 - Three-phase comprising the three possible wetting states	24
Figure 12 – Two stages of spreading of a silicone drop on a glass substrate: (a) $t=3,25s$ after deposition, (b) $t=18,25s$ after deposition	25
Figure 13 – Comparison of contact angle evolution in Wetting and Dewetting transitions [18]	26
Figure 14 – Factorial experiment with two factors (left); Factorial experiment with interaction (right)[20]	27
Figure 15 – Factorial experiment, no interaction (left); Factorial experiment with interaction (right)[20]	28
Figure 16 – Scheme of dam material and LOCA in display device with Optical Bonding	30
Figure 17 – Display tare after dam dispensing (left); Manual assembly jig opened with glass cover (right)	31
Figure 18 – Manual dispenser of OB with static mixer (left); Quantity measurement of OB in scale (right)	31

Figure 19 – Dispensing of OB material in display (left); Manual assembly jig opened with display and cover layers (right)	32
Figure 20- Assembly of both layers until 1st point of contact (left); Spreading of Optical Bonding after releasing glass layer (right).....	32
Figure 21 – Schematic conceptual test of the dewetting effect	39
Figure 22 – Base structure with standard aluminum profiles (left); Base structure with support pillars for air curtains (right).....	49
Figure 23 – Heater group fixed in base structure (left); Air curtains connected to a Racor ¼ G/12mm (right).....	50
Figure 24 – Air curtains supports fixed to the base structure (left); piping installed in the heater nozzle (right).....	50
Figure 25 – Air curtains installed in the piping and fixed to the air curtains supports (left); Isometric view of the system (right).....	51
Figure 26 – Real system without insulation (up); Real system complet (down).....	51
Figure 27 – Instrumented system (left); Termopair in heater nozzle (right)	52
Figure 28 – Two termopairs in left air curtain (left); Three termopairs in right air curtain (right).....	53
Figure 29 - Termoprofile of OCS version 1 with potentiometer of heater set in level 2 scheme of instrumentation.....	54
Figure 30 - Termoprofile of OCS version 1 with potentiometer of heater set in level 6 scheme of instrumentation.....	55
Figure 31 - OCS version 2	56
Figure 32 – OCS version 2 instrumented (left); termopairs in the affected corners of display (right).....	56
Figure 33 - Analysis of OCS version 2 with working continuously for a 15 min period with heater set to 5	57
Figure 34 - Temperature profile of OCS monitoring temperature in the corners of display....	59
Figure 35 – 3D model of product supports comprising four corner pillars	61
Figure 36 - Schematic of the FDM process	62
Figure 37 – FDM machine tool settings	63

Figure 38 – Layer settings on FDM machine	63
Figure 39 – Infill settings on FDM machine	64
Figure 40 – Representation of infill layers	65
Figure 41 – Main effects plot for response	71
Figure 42 - Interaction plot for response	71
Figure 43 - Pareto chart of standardized effects	74
Figure 44 – Plot of residuals vs temp (left); Plot of residuals vs time (right)	75
Figure 45 – Summary report of Anderson-Darling Test on the residuals data.....	75
Figure 46 – Triple overflow cure system setup	77

List of Tables

Table 1 - Results of cure time in terms of cure temperature and heat rate	20
Table 2 – Input parameters for DOE of overflow cure	34
Table 3 – L9 Orthogonal array selected for the study	34
Table 4 – DOE for the overflow cure study	35
Table 5 – DOE for the study comprising repetition runs and results evaluation method	36
Table 6 – Low surface energy materials used in the overflow dewetting tests	40
Table 7 – Input parameters for DOE of overflow dewetting	41
Table 8 – L5 array used in the study	42
Table 9 . DOE for the overflow dewetting study	42
Table 10 – DOE for concept surface deactivation plasma treatment	43
Table 11 – List of components	48
Table 12 – Description of the measurement in the response	67
Table 13 – Results of overflow cure experiment	68
Table 14 – 2D analysis of OCS tests	69
Table 15 - Design Summary and Factor Information (from Minitab)	70
Table 16 – Errors for each run of the DOE	73
Table 17 – Analysis of Variance (from Minitab)	74
Table 18 - Descriptive Statistics of the residuals (from Minitab)	76

1. Introduction

The project described in this dissertation took place in Bosch Car Multimedia in Braga, which represent one of the most important plants working in the automotive industry in Portugal, and as matter fact, it represents a significant part of the CM sector in Europe.

1.1 Project background and motivation

The project started because of a problem derivate from overflow of a liquid substance (LOCA) during assembly of two solid layers (comprising glass cover and display), through a process of Optical Bonding in the IS product shown in Figure 1.



Figure 1 – IS product for motorcycles produced by Bosch CM

Once the LOCA overflows out of the active area of the display to gaps external to the active area, it might get inside the lower part of the display, hence it may reach some electronic components of the product and cause their failure after the LOCA cures. This problem is displayed in Figure 2 of the next page. Some products assembled with this process are not affected by overflow of LOCA since the higher quality of the insulation tape placed between the inner and outer sides of the display prevents this from happening. Nevertheless, the more

different products are made with different components within this process, the greater is the probability of unexpected problems happening due to variations in the quality of the product.



Figure 2 – Infiltration of LOCA in the interior of the display

The major motivation and goal of the project is to achieve an automatized solution that eliminates the rejection due to this problem, that might be suitable to adapt for other products, in the event of this problem appearing again in the future.

1.2 The project at Bosch Car Multimedia

The project was developed at Bosch Car Multimedia in Braga which is one of the major suppliers of CM products in the automotive industry, and responsible for most of the innovation observed in this sector for the last years. Bosch Production System, BPS, establishes a standard for production where OEE must be above 90%. Whenever OEE climbs down this value a strategy needs to be developed, and actions must be taken in order to get it back above the minimum level of 90%. To do so, a detailed diagnose should be done to find what the root problem is.

The departments involved in this process analysis were CM/MFT5 and MFT/MTN, which correspond to sections of Process Development and Maintenance. Both departments combined have theoretical knowledge, field experience, know-how and previous experiences working together.

This project took shape after the problem described in chapter 1.1 was found, due to a new product with components of different quality regarding the insulation tape in a Optical Bonding process. The relevance of this project is to create a solution that allows the manufacturing process to control overflow and eliminate the problems arising from it, no matter the products assembled in the process.

1.3 Methodology and structure of dissertation

The methodology is described early in this section and its phases are schematically represented in Figure 3.

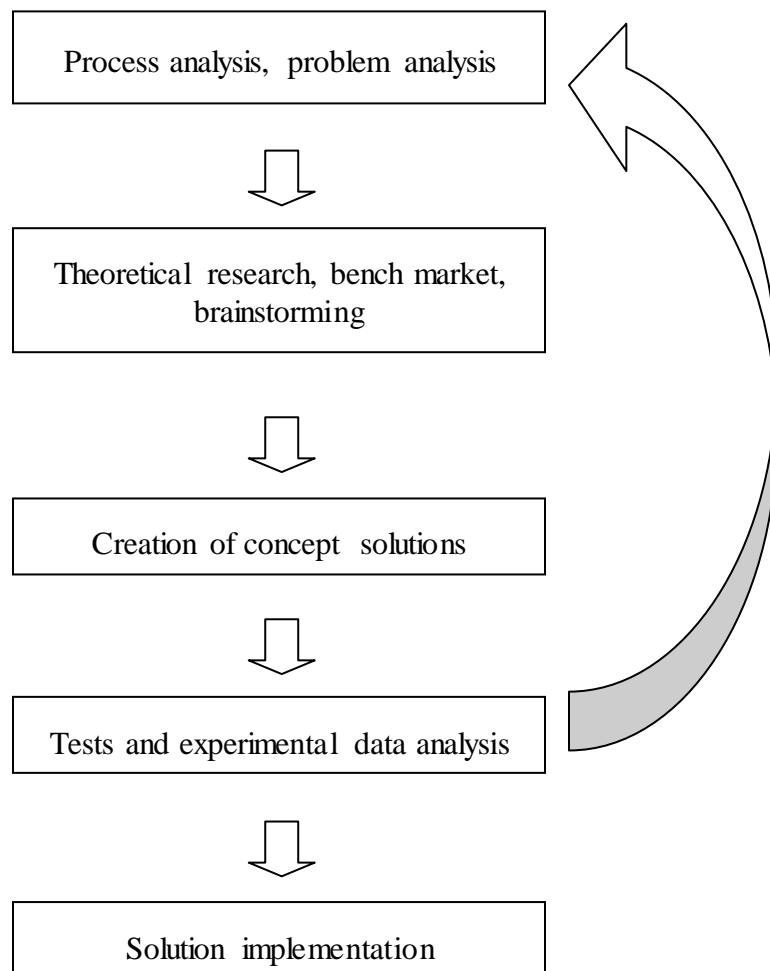


Figure 3 – Methodology diagram

The first phase consists in thoroughly analyze the process and the problem that the study aims.

After identifying the subjects of interest the phase that follows comprises bibliographic review, market research and brainstorming to balance the possible options available to conceive a solution, based on the experience and knowledge about the process and theoretical concepts previously investigated.

The next phase is the creation of one or more concept solutions that may be viable. This decision is highly dependent of all the requirements of the products and processes involved. Also, the failure modes of the solution/system need to be prevented to a maximum, because if the test conditions can't be guaranteed as near ideal the results are not reliable a solution to be implemented in the industrial process. If tests deliver unsatisfactory results the second phase must be addressed again to rethink the problem, as shown in Figure 3.

Finally the ultimate phase is to implement a viable solution. In this last step of the project, the solution is ready to be implemented, but nevertheless it needs to be upgraded so it can work properly in continuous production, complying to the respective norms and standards, as well as it needs to assure process capability, capacity and product requirements.

The structure of the dissertation is summarized in the paragraphs bellow.

Within Chapter 1, this master thesis starts with a presentation of the project's origin, as well as an introduction of the company and the many parties that were somehow involved in the project development.

The state of the art is presented in Chapter 2. In this section several different fields of study are addressed. This is multidisciplinary information that represents the basis of each of the solutions developed or tested. The theoretical data required to conceive each solution is thoroughly explored in this section. In practice, one intends to provide concepts, terms, equations or any complementary theoretical information that are essential for the development of the project.

Further in the dissertation, along Chapter 3, the DOE is presented for the experiment with the OCS, prototype machine created for this solution, and for the conceptual experiment of a surface deactivation plasma treatment. The test parameters are carefully identified for both solutions. Further in this chapter either constant parameters as input factors are defined, resulting in a DOE for each solution. Also the procedure of the tests is thoroughly explained along this chapter.

Therefore, in Chapter 4 the design of the experimental setup is explained. This section comprises most of the technical data related to components selection, prototype assembly, working conditions and the remaining information that is relevant for the design of the

experimental setup and its analysis. Both solutions presented in this dissertation were developed in a short amount of time, which proved to be a limiting factor. The demanding situation was aggravated due to delays in delivery of material, a factor external to the company. For this reason only one of the solutions was possible to materialize, and only that solution is presented in this chapter.

After performing the tests, within Chapter 5, there is the discussion, statistical analysis and finally conclusion about the results. It is possible to have either tendencies, inconclusive results or failure in a test. Although the goal of the dissertation is to actually bring satisfactory results to discussion so that is possible to restrain the problem, even failure allow to conclude that a certain idea is not functional or at least not without the proper changings/upgrades.

Inside Chapter 6 of this dissertation there is a presentation of the conclusions that arise from the project along all phases of its development.

In the end of the document one can find the references and attachments relevant to the project.

1.4 Project goals

The project aims to create a solution that guarantee OEE values never bellow 90% due to this problem previously identified in this dissertation. As previously stated, the priority is to find an automatized solution. Therefore, the main and secondary goals for this project are:

1. Find an automatized solution that eliminates rejection in the Optical Bonding process due to overflow of LOCA from the active area to the interior of the display;
2. Understand this process of Optical Bonding in terms of:
 - a. Cure reaction of the LOCA;
 - b. Wetting and spreading phenomena.

Nevertheless, it must be sustainable in terms of:

- Process and product specifications: The norms established for the process and product must be respected, and any specification that is already defined must not be changed.
- Budget: The solution is only reliable and acceptable if it overcomes the problem within a short budget comparing to the loss that the problem represents in terms of production;
- Process sustainability: The solution cannot increase the current cycle time of the production line. The less it affects the line of production, the better it is.

- Materials and resources: New materials applied to the product should be avoided, as well as the available resources in the production line are desirable rather than new technologies.

Each of the solutions presented in this dissertation are designed regarding the guidelines previously stated.

Although this work presents two DOE and one solution are based on quite simple concepts, it required a lot of time and persistence in terms of research, experimental work, and analysis to create evidence that might if the ideas suggested are fit for a solution.

2. State of the art

In order to reach an effective and economically viable solution, the problem was widely studied, in order to tackle it from different points of view. The objective and importance of this theoretical review is to better know the problem and hence come up with an effective and reliable solution. Along this chapter the relevant data that has been reviewed will be shown in the required level of detail that is needed for the project at hand.

Firstly, it is presented the concept of Optical Bonding and some properties of an Optical Bonding process.

The thermal properties of the LOCA were previously studied. The strategy adopted is monitoring the evolution of viscosity with time for different cure temperatures, so one can better understand the cure process of the material that infiltrates the display assembled in the process.

Another field of study explored is spreading and wetting. For the last two decades the increase of knowledge in this area was large, mostly thanks to the growth of the adhesives industry. One of the most critical factors to take into account when performing an adhesive joint is the wettability of the bonding material in the surfaces to bond. Wettability is measured through contact angle [1]. A given liquid material can wet differently a given solid surface, depending on the free energy of that same surface.

2.1 Optical Bonding

The increasing number of digital Car Multimedia products used in the automotive industry resulted in a huge development of these products over the last decade aiming for enhanced optical properties, among others.

The Optical Bonding process appeared in industry as a solution to tackle this issue. It's a process that eliminates the air gap between glass cover and display, resulting in the reduction of reflections and elimination of the refraction index between solid layers and the mid gap that exists between glass cover and display device and typically filled with air [2]. The comparison of these phenomena in display devices without bonding and with bonding is schematically represented in Figure 4. In a simple explanation, Optical Bonding is the process of laminating two layers of a display device using optically clear adhesive (OCA) in the volume where the air gap would be. The OCA used in an Optical Bonding process may be silicone based materials, urethane based materials, among others. The common goal of these materials is to enhance the optical properties of a display device that are previously referred in this chapter.

As previously stated, Optical Bonding reduces reflection by eliminating internal reflection between display and glass cover. This is achieved because this bonding process creates a single index of refraction across these layers, hence reducing internally reflected light loss and increasing display contrast and viewability [3]. Improved display contrast enables the display to be more readily seen in bright ambient conditions, which is a rather important characteristic for the CM industry.

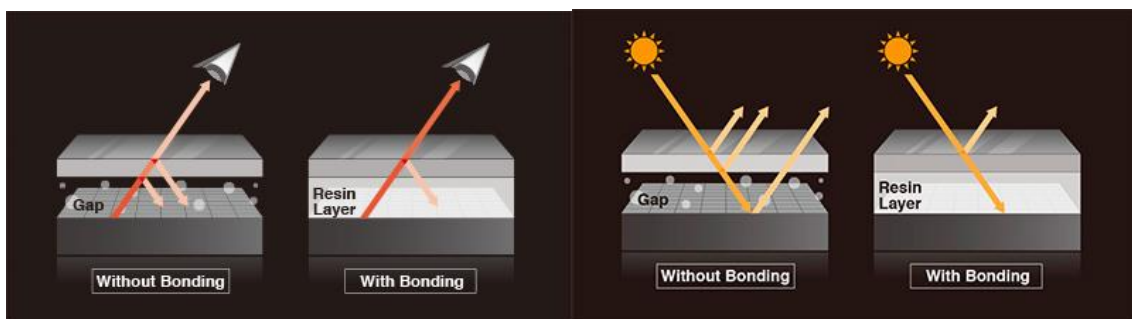


Figure 4 – Schematic comparison of Optical Bonding and air gap in terms of: light loss (left) and glare (right) [4]

Also it enhances some other properties of the product, namely the increased bonding strength and the protection against dust and moisture. This represents protection from external factors that can cause the display to be unreadable. When compared to a similar product without Optical Bonding, the products subjected to this process are more resistant and normally the life cycle of the display is longer. The process itself only alters the surface of the display rather than its components, without interfering with the display's operating range of temperatures.

Bearing in mind that the display is sensitive to Electro Static Discharge (ESD) and that contamination of the visible area before the end of assembly will cause rejection, the process must be undertaken in a low ESD and clean room environment. The Figure 5 illustrates a modular clean room ISO 5. [5]



Figure 5 – Example of clean room (ValuLine Hardwall Modular Cleanroom)

Within Optical Bonding processes, the main differences that may appear between one type and another are mostly how the thickness of the bonding layer is controlled, the technique used to assemble glass cover and display. Also which kind of adhesive is used to perform the Optical Bonding is a variable, as well as the design of the air vents [6].

In order to achieve the desired results from the Optical Bonding, it is important to assure full surface contact with the adhesive before the cure reaction starts, to guarantee both bond strength and optical properties without air bubbles or contaminations. For this reason normally there is a surface treatment in one of the layers, in order to control and enhance the spreading of the LOCA.

The process can be divided into five different phases, consisting of preparation of glass cover and LCD layer, application of adhesive in one of the solid surfaces to bond, alignment of both glass cover or touch screen and display, Lamination of display and glass cover with Optical Bonding, preparation of product for delivery to client. This represents the conceptual steps behind a process of Optical Bonding. Figure 6 represents schematically an Optical Bonding

process which consists in Dry Film Lamination, resorting to a pressure sensitive adhesive (PSA) with visco-elastic behavior, that also stands for the concept of Optical Bonding processes in general. [7]

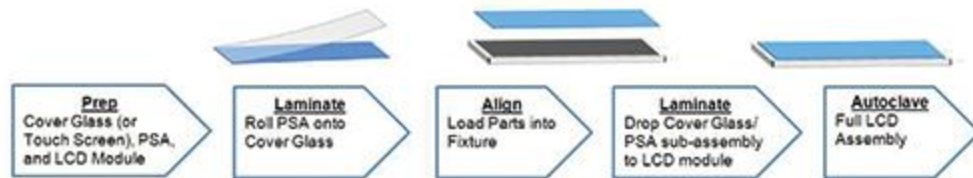


Figure 6 - - Scheme of Direct Dry Film Optical Bonding [7]

Preparation of the surfaces also depends on the OCA to be used. It is always mandatory that both surfaces are deeply clean, which normally requires a cleaning process already within a clean room environment. Surface treatments may be used to control how an adhesive spreads and makes the contact with a given surface. The LOCA has to be chosen accordingly to a given product or process. Thereby this material is required to be optically transparent, to keep its properties over time and to have a suitable refractive index that matches the refractive index of both cover glass and display surface [7]. The alignment is achieved with vision software being that both cover glass and display are assembled and laminated right after alignment. The assembly operation may be performed in different ways, but normally one of the parts stay fixed so that the order is aligned hence assembled. The last step is testing and autoclave to further be delivered to the client. [7]

Even when a standard Optical Bonding process is already implemented and stable there is the need to have alternate solutions to face unexpected problems. These situations can happen due to variability in components supply or lower quality of the components of a given product, when compared to the product for which the process is stable.

This project aims to absorb some of these variations in the process, through developing an additional mid step inside the Optical Bonding process that controls the overflow of the liquid adhesive, in case it happens. Beyond avoiding the contamination of the components that can't be in contact with the LOCA, this additional step helps maintaining more accurately the amount of it that is kept in the active area, as a consequence of controlling the overflow.

2.2 LOCA

This section shows some studies with the dual component silicon based LOCA used as bonding material in the process, in order to understand its rheological behavior and how the overflow problem should be addressed. This data is part of the *lessons learned* documents of the company. The objective of these studies was to characterize the material and thus optimize some features of the process, being that the test parameters and conditions were defined for previous works. In this work this data is used to design a modification to the process if it is supported by a positive expected result. However the information provided in the following paragraphs doesn't represent all of the operating range of temperatures of the product, it is possible to predict a hypothesis beyond the minimum or the maximum limits of the tendencies. To achieve this knowledge the fluids were tested with DSC (Differential Scanning Calorimetry) and reometry tests. Therefore the most important variables to study are the time necessary to trigger the cure process and its cure time (to achieve 100% curing) for a given cure temperature. Nonetheless, a complete cure profile should be acknowledged, since cure reactions are associated with increase of viscosity that is detectable by reometry and also enthalpy variations detectable by DCS.

At first, the tests conditions consisted in heating the material from 24 °C to 120 °C using four different heat rates, 2 °C/min, 5 °C/min, 10 °C/min and 20 °C/min. The heat rates used in the tests are constant so that the effects of thermal inertia are avoided and hence can be despised.

The Figure 7 was exported from a not editable document, and for this reason the language and notation are not according to the rest of the dissertation. On the left, bottom and right axis refer to percentage of cure, time and viscosity respectively

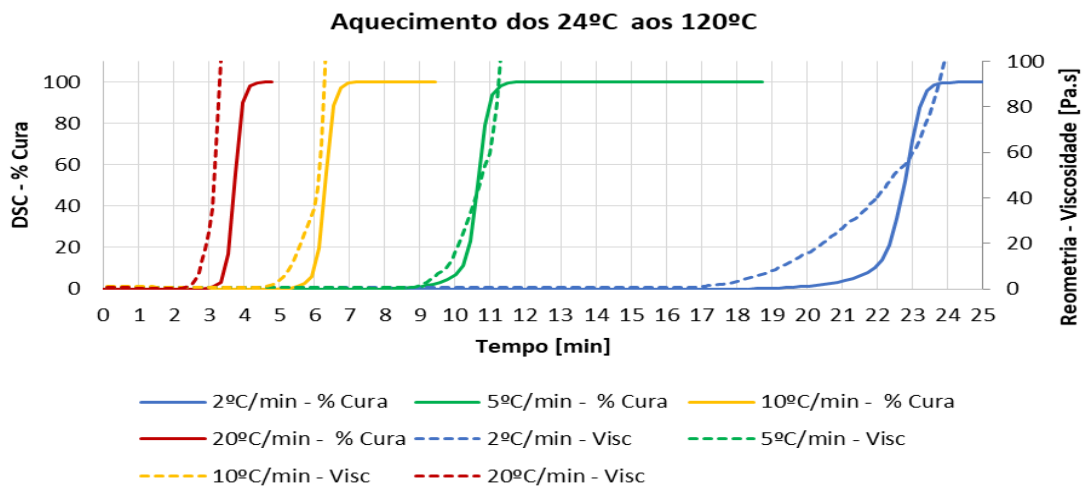


Figure 7 – DSC tests heating LOCA from 24°C to 120°C changing the heat rate

In Figure 7 one can find the results of these tests where the dashed lines represent material viscosity determined through reometry tests and the continuous lines represent the percentage of cure along time, resulting from DSC.

As a prior analysis one can say that in both techniques the cure reaction is irreversible and that the cure starts at similar times on both techniques, as expected. Therefore, it's observable that when the material is exposed to different heat rates, the start time of the cure reaction varies. Thus, a higher the heat rate will result in an early start of the reaction. Nonetheless, the gradient observed in the viscosity curves grows with increase of heat rate. Having this stated, one can conclude that higher heat rates will result in faster cure reactions.

Usually, a cure process in industrial environment has a defined cure temperature. In order to study the influence of the cure temperature in the cure process, isothermal tests were performed measuring the cure time of the material for different cure temperatures and different heat rates. These tests were conducted resorting to DSC because of the capability of its oven to better control temperature.

The tests combined cure temperatures from 50 °C to 70 °C with an increment of 5 °C, with heat rates of 10 °C/min, 25 °C/min, 50 °C/min and 100 °C/min. The results are shown in the Table 1 and Figure 8 of the next page. The adhesive takes too long to start curing at environment temperature, for this reason the chosen temperatures for the test are significantly greater than 25 °C.

Table 1 - Results of cure time in terms of cure temperature and heat rate

Cure Temperature	50 °C	55 °C	60 °C	65 °C	70 °C
Heat Rate					
10 °C/min	39 min	24 min	17 min	9 min	8 min
25 °C/min	36 min	24 min	15 min	8 min	6 min
50 °C/min	37 min	23 min	13 min	7 min	6 min
100 °C/min	35 min	21 min	13 min	6 min	5 min

The tests performed allow to conclude that time needed to cure the material decreases exponentially with an increasing cure temperature, regardless the heat rate applied to heat the

material. For example, taking into account the heat rate of 100 °C/min wherein the cure temperature (isothermal stage) is 50 °C the material takes 35 min to start curing, but for cure temperatures of 60 °C and 70 °C it takes 13 min and 5 min respectively, for the same heat rate.

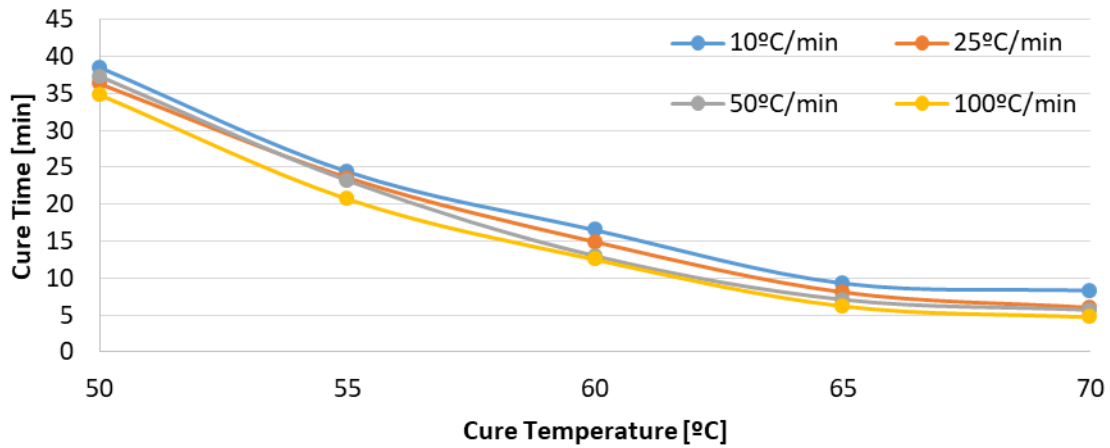


Figure 8 - Cure time of silicon A as a function of cure temperature for different heat rates

On the other hand, the different heat rates used have direct influence in the cure time, where lower heat rates only delay the start of the cure proportionally to the additional time that it needs to reach the cure temperature, when compared to higher heat rates. Having the 50 °C temperature as example, with an heat rate of 10 °C/min the sample needs 3 min, as one can observe in Figure 7, to reach the cure temperature and in this conditions it cures in 39 min, as one can observe in Figure 8, while for a heat rate of 25 °C/min it needs 42 sec to reach the cure temperature and approximately 36 min to cure. This represents the offset between the lines of the chart, since 2 min is approximately the difference between both cure times.

The tendency indicates that it is possible to cure the material in less than 5 min or less, if higher heat rates are used along with cure temperatures equal or higher than 70 °C.

The rheometry tests, used to confirm the previous results, were conducted regardless the heat rate because of the oven being sensitive to temperature overshoots, as high as the heat rates used. To overcome this obstacle, these tests in the rheometer were conducted in the isothermal stage only, letting the oven heat until the desired temperature and only then placing the samples in rheometer. Since the material is placed in the rheometer until the values of viscosity start being registered, a time gap passes. This time, necessary to prepare the sample and the test, is usually of 4 min while the material is already exposed to high temperatures, so it needs to be acknowledged as part of the cure time.

The Figure 9 represents the changes in viscosity along time for cure temperatures of 65 °C and 70 °C. As one can observe in this figure, when the cure temperature used is set to 70 °C, the cure already started by the time viscosity values start being registered. The cure reaction is expected to start approximately 5 min after the samples are in the oven. As previously stated, the sample tested in an isothermal stage of 70 °C is already curing when values start being registered, which is explained with preparation time required for each sample, of 4 minutes. In the isothermal stage of 65 °C the material starts curing 2 min after values start being registered. Summing the 4 min of sample preparation it corresponds to the expected 6 min until the cure reaction starts. The same conclusions from two different techniques ensure that these are reliable results.

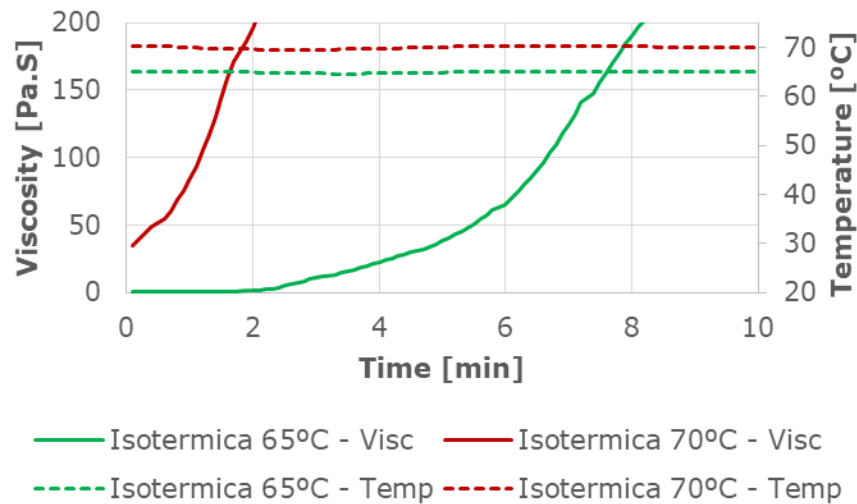


Figure 9 – Evolution of viscosity of the material with time for different cure temperatures

This knowledge is complementary to the information given by the supplier, since this adhesive was first designed for a specific cure temperature and time. All the experimental data reviewed in this sub chapter comprises the base knowledge used to define the variables in the tests of Overflow Cure System (OCS). These test parameters are further detailed in the DOE available in Chapter 3.

2.3 Wetting and spreading

Within this section the theoretical basis of wetting phenomena is reviewed, further used to conceive a dewetting effect through applying a surface deactivation plasma treatment.

At first, there will be shown an explanation of the basic concepts involved in the wetting and spreading phenomena, followed by a review on surface energy and contact angle is done and measurement of this properties.

The wetting phenomenon is an area where chemistry, physics and engineering intersect.

The most important and most studied part of this phenomena is related to surface chemistry. For the last years many research has been devoted in determining wetting behavior and how to control surface properties that may change it [8]. To achieve specific wetting properties one of the most important factors is surface energy which will dictate the way a fluid spreads over a solid surface. Changing the chemical properties of the surface of a material, one will change the contact of the surface with liquids, vapors or solids. Nowadays the most commonly used chemical means to do this are silanization [9] and plasma treatment [10].

Wetting and spreading are governed by surface and interfacial interactions acting in small (nanometers scale) or molecular distances. The equilibrium of forces derivate from the contact of a liquid with a solid surface, resulting in a contact angle θ , as displayed in the Figure 10 bellow. In the force equilibrium, three surface tensions need to be considered: the interfacial tension between solid liquid γ_{sl} , the surface tension of the liquid γ_{lv} , and the surface free energy of the solid γ_{sv} . [11].

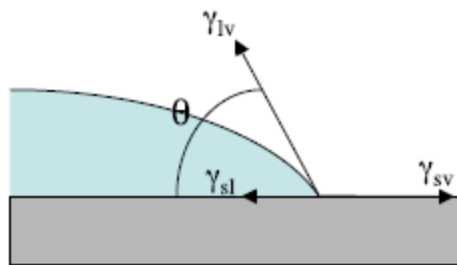


Figure 10 – Representation of acting forces on the contact line between a solid and a liquid layer [1]

These tensions originated at the first instant of contact, are balanced in Young's equation shown below [12]. With this in mind, one can state that a variation of the surface tension of liquid or solid surface will cause the contact angle to change.

$$\gamma_{SV} = \gamma_{SL} + \gamma_{LV} \cdot \cos \theta_{eq} \quad (1)$$

In the relation expressed in Young's equation (1) the kinetics involved will vary until the equilibrium is reached. Mathematically speaking, the distinction between the different wetting states is usually made by considering the equilibrium spreading coefficient $S_{eq} \leq 0$, which represents the surface free energy γ_{SV} relative to its value for complete wetting. Focusing on wetting, if $\gamma_{SV} < \gamma_{SL} + \gamma_{LV}$ a droplet with a finite contact angle minimizes the free energy of the system resulting in partial wetting. On the other hand if $\gamma_{SV} = \gamma_{SL} + \gamma_{LV}$ the contact angle is zero and the resulting equilibrium state is complete wetting.

$$S_{eq} = \gamma_{SV} - (\gamma_{SL} + \gamma_{LV}) \quad (2)$$

$$S_{eq} = \gamma_{LV}(\cos \theta_{eq} - 1) \quad (3)$$

In Figure 11, a three-system is identified through variation of the surface tensions and hence contact angle variation. It's important to be aware that in most of the cases, the wetting phenomena is not in equilibrium, so the experimental work will focus mostly on the transitions between states.

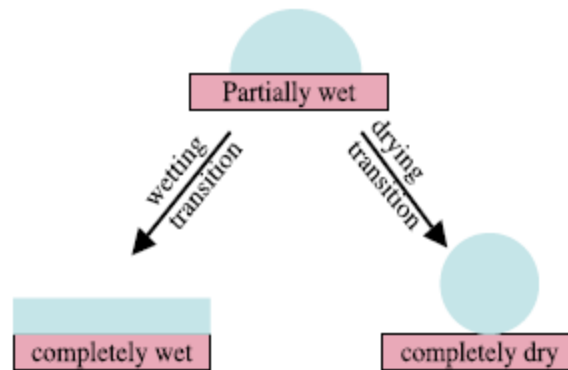


Figure 11 - Three-phase comprising the three possible wetting states

This representation shows the three wetting states that may exist in any three-phase system. For a solid-liquid-vapor system, complete drying would correspond to the intrusion of a macroscopic vapor layer between the solid and the liquid, thus “drying” does not imply evaporation. From a thermodynamic point of view, the wetting and drying states are very similar, the only difference being that liquid and vapor are interchanged. In practice, drying is rather rare, noting for instance, glass is a notable exception with mercury on, since van der Waals forces tend to thin vapor layers. So the focus here will be on wetting. Partial wetting corresponds to drops, surrounded by a microscopically thin film adsorbed at the surface, and complete wetting to a macroscopically thick layer. This can be observed in Figure 12, where

the evolution of a drop that is laid upon a glass substrate which it wets completely is captured in two different instants. As the drop spreads towards equilibrium the contact angle tends to zero.

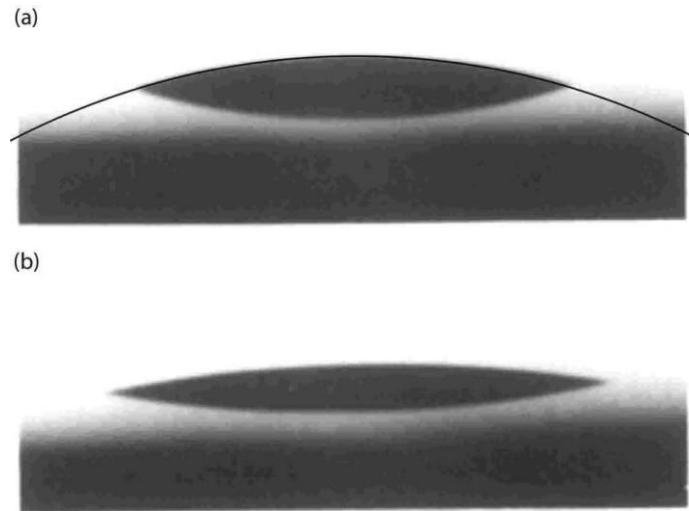


Figure 12 – Two stages of spreading of a silicone drop on a glass substrate: (a) $t=3.25s$ after deposition, (b) $t=18.25s$ after deposition

Thus, in a partial wetting state the surface apart from the droplet is never completely dry. In thermodynamic equilibrium there will be at least some molecules adsorbed onto the substrate, since the entropy gained by the system in doing this is large. It is for this reason that it is considered a microscopic film, in experiments the average thickness of this film varies between a fraction of a molecule to several molecules, depending on the affinity of the molecules for the substrate, and the distance to the bulk critical point. For complete wetting the equilibrium spreading coefficient is zero. The solid-vapor interface then consists of a macroscopically thick wetting layer, so that its tension is equal to the sum of the solid-liquid and liquid-vapor surface tensions. However, when a droplet is deposited on a dry substrate, it is hardly ever in equilibrium. Moreover, when studying the wetting behaviour of liquid it is important to make the distinction if it is volatile [13] or nonvolatile [14]; [15].

On the opposite hand, of wetting there is the dewetting. In many recent experiments and applications a uniform liquid layer is laid down on a solid that it does not wet [16, 17]. As a consequence of the non-wetting properties, the film may destabilize to expose “dry” patches, unless it is sufficiently thick to be stabilized by gravity [15]. The Figure 13 in the next page shows the difference between the wetting and dewetting transitions in terms of evolution of the contact angle.

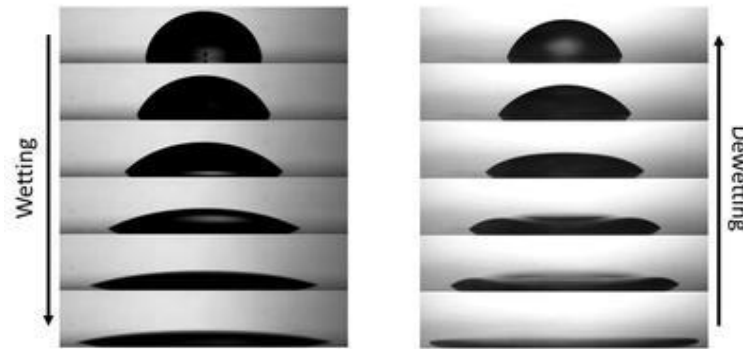


Figure 13 – Comparison of contact angle evolution in Wetting and Dewetting transitions [18]

The initial nucleus that give shape to the holes can either be caused by surface heterogeneities or dust particles, as well as thermal noise perturbing the system. These cases are “heterogeneous nucleation” and “homogeneous nucleation” respectively. In both cases the system gets separated from its equilibrium state since opening a small hole in the liquid layer “costs” more energy than is gained by thinning the film. For sufficiently thin films where long-range forces gain importance, the system can become linearly unstable, where one observes thermal fluctuations growing and hence spontaneous destabilization. This case has been called spinodal dewetting in analogy to the spontaneous decomposition of incompatible bulk phases [19]. Therefore, one can state that if a liquid is deposited on a low energy solid surface (sufficiently low so that the liquid does not wet it) it will attempt to form dry zones, causing the contact line to recede. However, gravity has great influence in the force balance, causing fluctuations if the film is thick enough.

2.4 Factorial DOE

When there are several factors of interest in an experiment, a fractional factorial design should be used.

In such designs factors are varied together. Specifically, by a factorial experiment we mean that in each complete trial or replicate of the experiment all possible combinations of the levels of the factors are investigated. Thus, if there are two factors A and B with a levels of factor A and b levels of factor B, then each replicate contains all $a \times b$ possible combinations. The effect of a factor is defined as the change in response produced by a change in the level of the factor. This is called a main effect because it refers to the primary factors in the study. An example will be shown, in order to introduced the concepts used for the DOE analysis in this

dissertation. Considering a factorial design with two factors and two levels each, both levels of factors “A” and “B” are denoted by “-” and “+.” These two levels are called “low” and “high” respectively. The main effect of factor A is the difference between the average response at the high level of A and the average response at the low level of A, or

$$A = \bar{Y}_{A+} - \bar{Y}_{A-}$$

After calculating the main effect of both it's possible to see which factor as more effect according to the average response of the factor with variation of the other factor [20].

Nevertheless in some experiments, the difference in response between the levels of one factor is not the same at all levels of the other factors. When this occurs, there is an interaction between the factors. To access if there is interaction between factors it is necessary to calculate the effect of a factor of each level of the other factor. In the example given previously this means that the effect of A for different B levels as to be calculated through the difference between the average value of A^+ and A^- for each of the B levels. Furthermore an analysis of two factorial experiments will be presented. In Figure 14 there are two factorial experiments, one with no interaction on the left and another with interaction of the right.

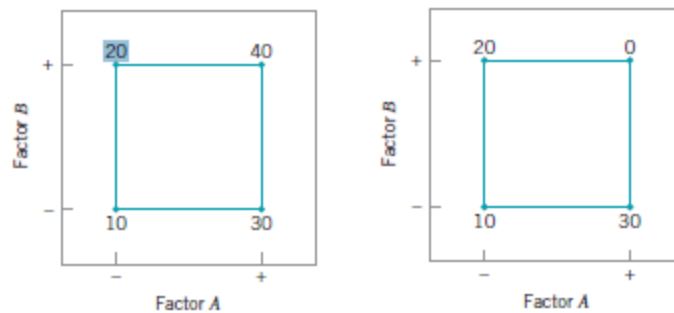


Figure 14 – Factorial experiment with two factors (left); Factorial experiment with interaction (right)[20]

In the first one (On the left of Figure 14) the main effect of A and B are 20 and 10 respectively, being that in the second experiment the main effect of A and B are 0 and -10 respectively. The first apparent conclusion is that in the first experiment the most influent factor in the experiment is A being that its main effect is twice bigger as the main effect of B. In the other experiment the main effect analysis leads to conclude that factor A doesn't influence the response.

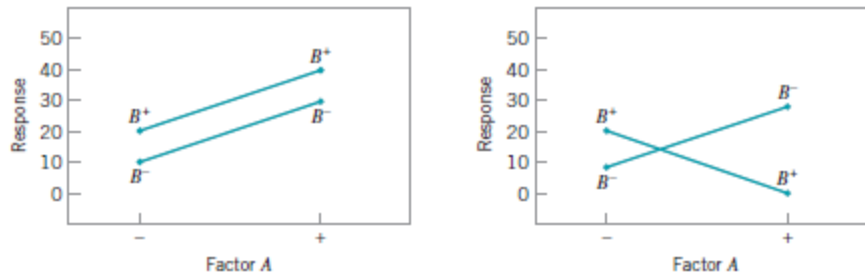


Figure 15 – Factorial experiment, no interaction (left); Factorial experiment with interaction (right)[20]

However, with the analysis of the influence of factor A in the response for different B levels provided on the right of Figure 15, it's possible to conclude that not only this factor influences the response rejecting the previous conclusion, but also that both factors interact. On the other hand the left side of Figure 15 reveals that in the first experiment the influence of factor A is independent of the level of factor B. [21]

Concerning how well the model represents the response for the experimental data or new observations, the values of S, R^2 , R^2 (adj), R^2 (pred) must be observed. The lower is the value of S the better the model fits the data. About the R^2 describes the amount of variation in the observed response values, R^2 (adj) is a modified R^2 which is adjusted for the number of terms in the model and in the presence of unnecessary terms while R^2 is artificially high R^2 is lower[22]. The value of R^2 (pred) shows how well the model can predict the response for new observations.

Furthermore, the results must be statistically validated. Through performing an analysis of variance to the factorial design, the p-value calculated for each effect can be compared with the value of α -level in order to determine if that effect is statistically significant. For a given effect or interaction if the p-value is less than α -level it has statistical meaning, therefore it is possible to conclude from the difference in the mean response among the different levels of that factor. On the other hand, if p-value is greater than α -level, than there is no evidence that differences in the average response depend on that effect or interaction. [22]

The residuals must also be evaluated in order to identify misleading results and how reliable the results are. For this matter, a descriptive statistics analysis of the results must be done in order to identify values like mean, standard deviation, minimum, median and maximum.

3. Design of experiment

The information within this chapter refers to the design and execution of the experimental work undertaken in the project.

For both of the experiments conducted, the early stage is to identify factors and constant parameters and thus define how many levels will be tested for those factors (number of variations). There are limitations in terms of budget, number of samples to be tested, time availability for testing, and test conditions for both experiments that are also described along the next subchapters. Every detail was thoroughly considered aiming to have a good balance between cost and quality/performance.

After identifying all input parameters and factors the tests are planned through a DOE.

Also the steps of each experiment are described, consisting of rules that guide the experimental work and that assure that each test is valid.

3.1 Overflow cure system

The factors identified for this experiment result from the rheological studies mentioned in the state of the art, and knowledge about the Optical Bonding process and the product requirements. Starting with the height where the air is dispensed that needs to be in conformity with the height where the glass and display are mounted. Nevertheless, the angular positioning of the air nozzles needs to be adjusted to the fixed position of the base structure that holds the kit with the work piece targeting the areas affected by the overflow of LOCA from below the glass. This way it is assured the repeatability of the process, once the kit with the sample is positioned in the base structure. Furthermore, feeding pressure and flow rate are factors that must be controlled through the pressure regulator and flow rate regulator valves of the pneumatic system. These factors must be set up in order to have the desired effect on the

temperature distribution in areas affected by overflow of LOCA, without interfering with the relative position of the glass and the display before the it is completely cured. The room temperature is kept at 20 °C that also respects the safety requisite of the heater, which can only be operated with environment temperatures below 60 °C (Attachment A – 1) .The experiment must respect the stages and requisites of both process and product. With this in mind, it is mandatory that all stages before, during and after dispensing the LOCA are strictly respected. To do so, the experiment resorts to one station in line to dispense the dam material and three stations that were prepared in the laboratorial set: manual assembly jig, overflow cure system and cure station. The dam material is the substance dispensed in the outline of the active area that defines the height of the bonding area as shown in Figure 16. Such as LOCA it is a dual component silicon based material.

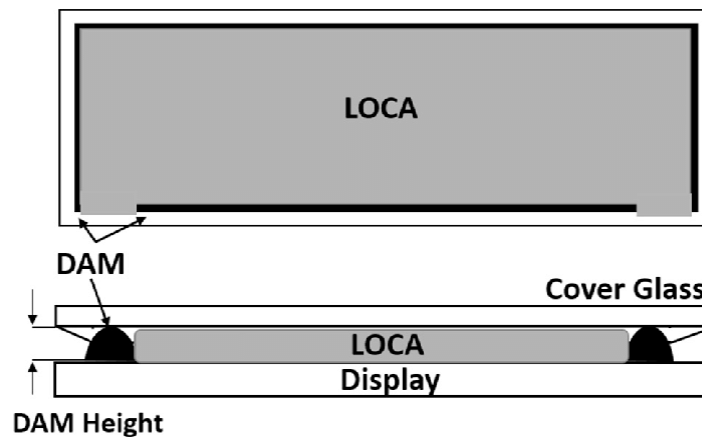


Figure 16 – Scheme of dam material and LOCA in display device with Optical Bonding

In order to let the air flow out of the active are during the assembly, there must be openings in the dam outline which are named *air vents*. As it is shown on the right side of Figure 17 in the next page, the manual assembly jig has to be opened and locked in that position, with the vacuum valve turned on and a sample of the glass cover fixed with vacuum between supports that assure positioning. The overflow cure system must be turned on respecting the previously stated factors and set for the temperature that is to be tested, monitored with the termopairs installed in the air nozzles of the system. Also before the experiment starts the cure station as to be set for 70 °C. In these two last stations of the laboratorial must be monitored until the operating temperature is stable, once this point is reached they are ready to operate. In regards to the dispensing of dam material it was decided to perform it in line, which allows to dispense with original dispensing program for the product that enhances the overflow of LOCA and represents the worst case scenario.

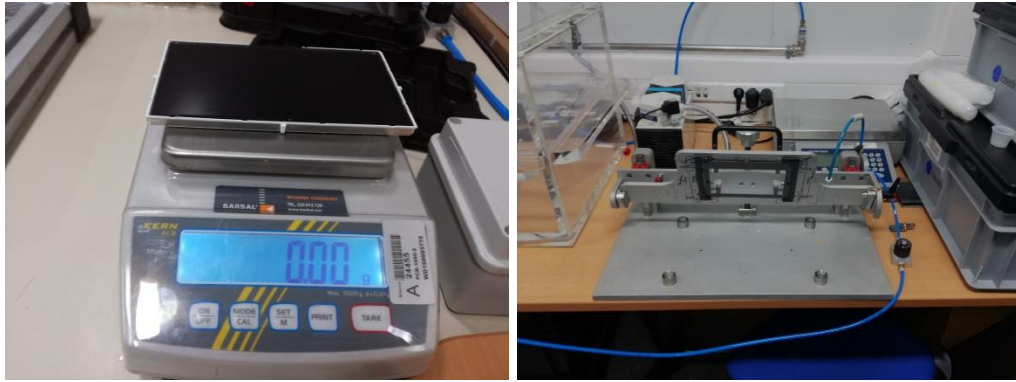


Figure 17 – Display tare after dam dispensing (left); Manual assembly jig opened with glass cover (right)

Another benefit of doing this step in line is that it can be controlled resorting to vision software thus ensuring accuracy in terms of positioning and quality of the lines dispensed, as well as quantity of material which is controlled by a scale.

After dam is dispensed on the display, it must be transported from the line to the laboratory so that the LOCA is dispensed within a time range of 12 minutes after dam is dispensed, time during which the dam material remains active, requisite defined the supplier of the product.

As in Figure 18, the LOCA is manually dispensed with the adequate static mixer, to a plastic cup controlling the quantity with a scale.



Figure 18 – Manual dispenser of OB with static mixer (left); Quantity measurement of OB in scale (right)

Furthermore, the material is manually dispensed in the display respecting the minimum amount of material and the V shape pattern. In addition the adhesive is dispensed on the display resorting to a precision scale where the tare of the display is measured enabling that one dispenses the right amount of material, with a precision of $\pm 3\%$. Then the display is

positioned in the kit and placed in the manual assembly jig. The described steps are shown in Figure 19.



Figure 19 – Dispensing of OB material in display (left); Manual assembly jig opened with display and cover layers (right)

The process continues within the manual assembly jig with three different phases: lower the glass layer until the first point of contact is established between adhesive and glass cover, decrease the angle until the LOCA spreads to the corners, close the vacuum valve releasing the glass and wait until the normal spreading is achieved in both sides. The Figure 20 displays the first and the final moments of the assembly part of the process.



Figure 20- Assembly of both layers until 1st point of contact (left); Spreading of Optical Bonding after releasing glass layer (right)

Following this stage, the kit is moved from the manual assembly jig to the Overflow Cure System base structure where the test position of the kit is already set. In this phase the temperature in the nozzles and time that the product is exposed to the hot stream is tightly controlled according to the parameterization of the test, being that in the end of the test the kit is taken from the Overflow Cure System and placed in the cure station where it will remain for 30 minutes at the cure temperature defined for the process. It is important to note that if the temperature of the oven is not adequate when the product leaves the previous station the whole test is invalid.

The input parameters for the test comprise two factors, with three levels each, likely to find a tendency, and are shown in the Table 2. The first factor is the temperature of the air in contact with the corners of the display where the cure of the LOCA is meant to be achieved. The second factor is the time of exposure, which is calculated concerning the time necessary to trigger the cure of the LOCA at a given temperature and the cycle time of the whole process.

In regards to the three levels of the factor temperature, the minimum temperature is 5 °C higher than the maximum temperature evaluated in the rheology tests of the LOCA, and that shows the best results in terms of enhancing the start of cure. Moreover, the maximum temperature of the tests is the maximum temperature that the display can stand from the product specification of the display in the Attachment A - 12. Given this, the minimum temperature of the experiment is 75 °C, also the maximum temperature 95 °C, being that the mid temperature is 85 °C which represents the middle value between the other two. Since the cycle time of the whole process is 3 minutes, the maximum cycle time that can be used in this station is also 3 minutes. Therefore, this time period stands for the minimum value to be tested in the time variable, as it is further explained in this section.

Concerning the LOCA used in this process, for a temperature of 70 °C the cure starts within 5, 6 or 8 minutes, the shortest time corresponds the maximum heating rate at the same temperature. Crossing this information, the first level of the time variable is the cycle time, 3 minutes, being that the other two are its multiples 6 minutes and 9 minutes. These values represent the setup of the process with a single station, two stations and three stations. This is materialized adding a conveyor to the production line right after assembly, guiding the product to two or three different stations where it would stage for 6 minutes or 9 minutes before it is transported back to the original path, rather than installing only one station in line. This way any parameterization can be applied to the process without becoming the bottle neck of the process.

Table 2 – Input parameters for DOE of overflow cure

Parameters	Level		
	1	2	3
Air Temperature (°C)	75	85	95
Time (min)	3	6	9

The possible combinations for the test variables are expressed on a L9 (3^2) orthogonal array, with the input parameters Temperature and Time expressed in Table 3. On the top of columns there are expressed both input parameters of the tests, being that the left cells of the line represent the number of iteration of the respective test. The filling cells comprise all three levels of the input parameters organized in a way that each experiment corresponds to one combination of the variables.

Table 3 – L9 Orthogonal array selected for the study

Experiment	Temperature	Time
1	1	1
2	2	1
3	3	1
4	1	2
5	2	2
6	3	2
7	1	3
8	2	3
9	3	3

Therefore, the resulting DOE is schematically represented in Table 4, using a similar L9 (3^2) array as in Table 3.

Table 4 – DOE for the overflow cure study

Experiment	Temperature	Time
1	75	03:00
2	85	03:00
3	95	03:00
4	75	06:00
5	85	06:00
6	95	06:00
7	75	09:00
8	85	09:00
9	95	09:00

In order to better understand and achieve more reliable results it was decided to perform three repetitions of tests for each set of parameters. Hence the number of tests will be $3^3 \times 3 = 27$. In Table 5 it presented a sheet of evaluation for this DOE, where the levels of the of the factors are already combined with space to fill the measured response and register observations.

Table 5 – DOE for the study comprising repetition runs and results evaluation method

			OVERVIEW (0-good; 3-bad)						OBSERVATIONS
Experiment	AIR TEMP	C TIME	IT	1st run	IT	2nd run	IT	3rd run	
1	75	03:00	11	-	12	-	13	-	
2	85	03:00	21	-	22	-	23	-	
3	95	03:00	31	-	32	-	33	-	
4	75	06:00	41	-	42	-	43	-	
5	85	06:00	51	-	52	-	53	-	
6	95	06:00	61	-	62	-	63	-	
7	75	09:00	71	-	72	-	73	-	
8	85	09:00	81	-	82	-	83	-	
9	95	09:00	91	-	92	-	93	-	

3.2 Concept low surface energy treatment

After reviewing the information relative to the basic concepts of the wetting and spreading phenomena, the goal is to design a solution that protects the areas where LOCA infiltrations occur using this knowledge. Thus, the objective of this surface treatment is to cause dewetting of LOCA in these areas. The solution proposed aims to assess if a surface deactivation plasma treatment is capable of cause dewetting of LOCA hence eliminating the problem. This is meant to be tested by simulating a deactivation plasma treatment though the application of a low surface energy coating in these areas. Since many of the treatments used to lower the surface energy of a given material cannot be employed in polymers (as most of the display's components), the viable options to test this idea would be the application of release agent coating or surface deactivation plasma treatment. Nonetheless the last one involves a big investment or outsourcing of this kind of equipment. For test's sake, it is proposed to use a release agent coating to evaluate if the predicted effect is possible to achieve. If the objective of the experiment is fulfilled the effect can be reproduced with a surface deactivation plasma machine.

Firstly, one protective frame is positioned above the display, leaving only the outer border visible, where one wants to apply the coating material. Then a thin layer of coating is applied in the previously referred areas. Afterwards, when the LOCA overflows the dam line, one expects it to be able to spread along the dam line rather than into the infiltration areas, because of the free energy differential between the LOCA and the coating material. In other words, the goal is to cause the contact angle to increase in the boundary line formed between LOCA and coating material, providing conditions for a dewetting phenomena pulling overflow back to further cure near the dam line, and keeping the product free of infiltrations.

To select the release agent, the following requirements must be respected:

- It must “release” silicon compounds such as LOCA;
- It must be inert to the LCD surface as well as the display's housing material;
- Working temperatures must be the same of the display, preferably it must cure at room temperature;
- Surface energy significantly lower than 36 mN/m which is the surface energy of the LOCA;
- It must not react with any of the dispensed materials (LOCA and dam material).

The experimental setup design to test this conceptual experiment is briefly explained bellow.

Although initially the concept was meant to be tested directly on the product, it would deliver poor information about the phenomena itself because it is difficult to replicate exactly the same pattern and assure the same adhesion of the release agent layer to the display frame, and also less information about its application to other products. As an alternate solution a conceptual test to assess the dewetting phenomena was developed and described further in this chapter.

A first analysis of the properties that might assess if the targeted effect is achieved, identified force equilibrium along contact line to be the most suitable evaluation measurement. Therefore, the surface tensions of solid-vapor, liquid-vapor and solid-liquid interactions must be considered, which dictate how the liquid wets the solid substrate, and one needs to consider the weight of the cover layer that mounts on the display during the Optical Bonding process.

Studies have shown how is the evolution of contact angle with an increasing radius of a drop deposited on a solid substrate, which can also be seen with mass increase of the drop [15, 23]. As mass increases, the effect of the surface tensions effect becomes less significant for the contact angle and hence spreading of the liquid [23]. Following this logic, the DOE aims to allow the evaluation if it is possible to cause dewetting when the glass weight is applied over the liquid by lowering the surface tension of the solid surface. Being that the failure outcome may represent either that the surface energy is not low enough or that the mass of the “drop” of LOCA is too big, making the surface tensions effect less significant.

For this matter, a solid substrate is treated with a low surface energy material in order to low its surface tension. This is performed through leaving a rectangular area untreated, so that LOCA wets this part “freely”. To simulate the glass weight on the liquid, a razor with the proportional weight is guided parallel to the solid surface where LOCA is dispensed with two vertical pillars on both ends.

The steps of the described experiment are displayed bellow:

1. initially the surface is treated with a low surface energy material outlining the area that can be wetted;
2. measurement of surface free energy in the coated areas
3. followed by liquid drop deposition of the LOCA in the center of the area to be wetted;
4. then release the razor upon the drop;

5. and finally evaluate of the dewetting effect (OK/NOK)

The sequence of these steps is displayed bellow on Figure 21.

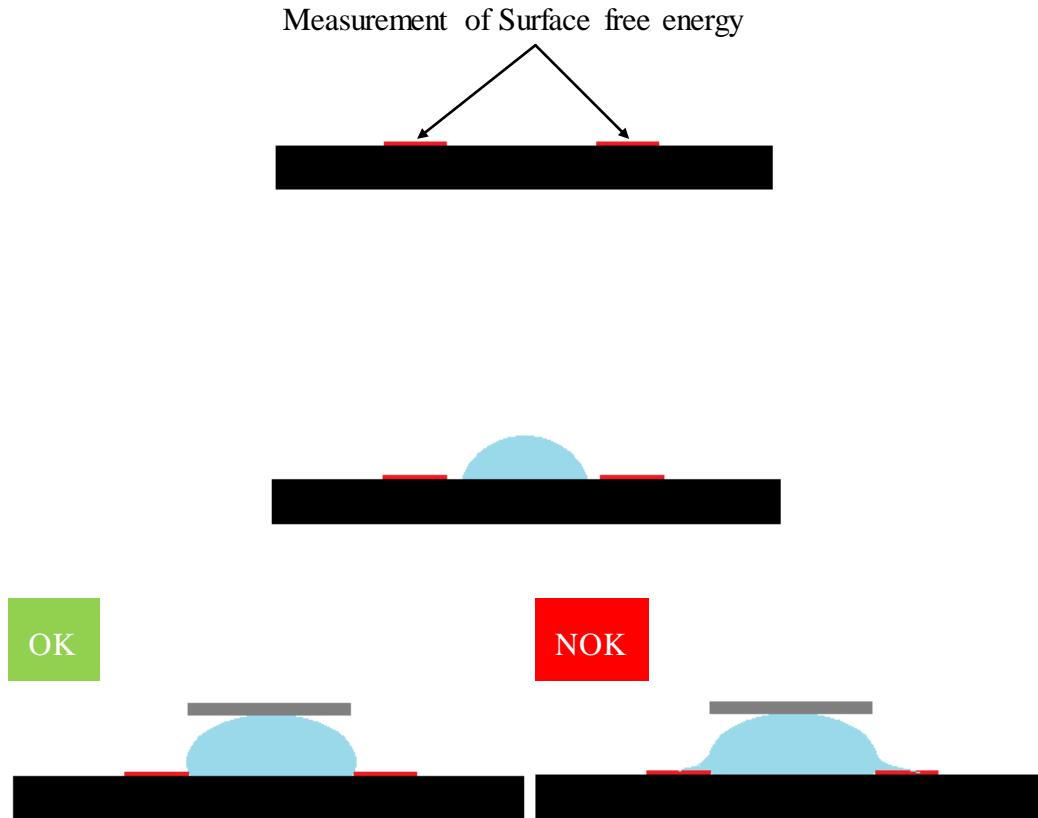


Figure 21 – Schematic conceptual test of the dewetting effect

After some research on the products available on the market that may be used to achieve the desired dewetting effect on the LOCA overflow, three different low surface energy materials were chosen to be tested, which are displayed in Table 6 present in the next page, along with the respective description and thickness if applied.

Table 6 – Low surface energy materials used in the overflow dewetting tests

Material	Description	Thickness (mm)
Loctite Frekote S50E	Water based release agent for silicone molds	N. A.
3M 5480 or 5481	Teflon tape	0,9
Tesa 4334	Acrylic adhesive compound tape	0,9

Taking a deep look into the materials, Loctite Frekote S50E is a release agent used to release silicone molds, and it's the best candidate among the three materials, due to its ability to release silicone based materials which is the case of the LOCA. This material is water based and once a layer is applied it needs to cure through water evaporation, which can be achieved drying for some minutes at room temperature. Although, the same material needs to be applied concerning air exhaustion and protection gear to avoid eye contact, skin contact and inhalation or ingestion for it is rather toxic. Also, the price higher than the other products, although it still is much cheaper than deactivation plasma machine, which one intends to simulate. On the other hand, both tapes shows low surface energy, and are the cheaper materials present in the study. Both 3M tapes shown in the Table 6 are made of teflon which revealed to be the material with lower surface energy among the most common materials available on the market. On the other hand, Tesa tape is used to outline painting areas, and as the special feature of preventing paint tears from trespassing it, and may as well perform the desired effect.

A DOE was designed for the conceptual tests to assess if the Surface Deactivation Plasma Treatment is capable of provoking dewetting of the overflow of LOCA, from the zones affected by this phenomenon. Therefore, the tests are performed resorting to a device with vertical guiding of a small horizontal plane surface, which will enter in contact with the LOCA, between the areas coated with a low surface energy material.

The constant parameters identified for this experiment are solid substrate composition, coated area, volume of the liquid drop, and also the weight and horizontal position of the razor that will compress the liquid drop. The solid substrate defined for the experiment is glass, due to its low roughness, enhancing the spreading phenomena. The volume of the liquid drop needs to be kept constant as well, this is done by weighing the liquid in a precision scale before

laying it on the solid substrate. The horizontal position of the razor has to be achieved by the vertical guiding, in order to simulate the dewetting effect as it is intended in the Optical Bonding process. Respecting the distance from the dam line until the gap where the liquid infiltrates, the area left uncoated is defined by a spacing of 2 mm between coatings. Also, the input factors are the low surface energy material which comprises three different materials and the coating layers. Although the number of layers is a factor of the experiment, it is not viable to apply more than one layer of any of the tapes because it would build a too high physical barrier, higher than the dam line, hence the results wouldn't evaluate the dewetting effect. Nonetheless three levels of the parameter "number of layers" will be tested for the Loctite Frekote S50E release agent.

Furthermore, the input parameters are displayed in the Table 7 display two factors, both with three levels, being that one of them will be tested only for one of the levels of the other factor.

Table 7 – Input parameters for DOE of overflow dewetting

Parameters	Experiments		
	1	2	3
Coating material	Loctite Frekote S50E	3M 5480	Tesa 4334
Number of layers	1	2	3

The combinations of the input parameters result in a L5 (3^2) orthogonal array as the shown in Tables 8 and 9 presented in the next page.

Table 8 – L5 array used in the study

Experiment	Coating material	Number of layers
1	1	1
2	1	2
3	1	3
4	2	N. A.
5	3	N. A.

The results of applying the input parameters values to the previous array, result in the DOE shown in table 9.

Table 9 . DOE for the overflow dewetting study

Experiment	Coating material	Number of layers
1	Loctite Frekote S50 E	1
2	Loctite Frekote S50 E	2
3	Loctite Frekote S50 E	3
4	3M 5480	N. A.
5	Tesa 4334	N. A.

As decided in the previous tests, three repetitions of each experiment will be performed in order to increase confidence in the results, also allowing a three point tendency for evaluations through measurement. The evaluation method for the study will consist in both contact angle measurements and resulting surface energy of the coated layer, resorting to

Kruss MSA, and visual evaluation of the dewetting effect. The number of tests to be performed is $(1 \times 3 + 2) \times 3 = 15$.

The resulting DOE is shown in Table 10.

Table 10 – DOE for concept surface deactivation plasma treatment

Experiment	Coating material	Number of layers	Surface energy (mN.m)			Dewetting effect (OK/NOK)		
			1st run	2nd run	3rd run	1st run	2nd run	3rd run
1	Loctite Frekote S50 E	1	-	-	-	-	-	-
2	Loctite Frekote S50 E	2	-	-	-	-	-	-
3	Loctite Frekote S50 E	3	-	-	-	-	-	-
4	3M 5480	N. A.	-	-	-	-	-	-
5	Tesa 4334	N. A,	-	-	-	-	-	-

4. Experimental setup

In this section, the experimental setups will be introduced. To project the setups, it is mandatory that all the requirements of product and process are respected, as well all the test conditions defined in the DOE. To do so, these conditions have to be identified in an early stage, so that each setup is correctly designed and its components selected in accordance.

The next subchapters will explain systematically each setup, where dimensions and selection of components are thoroughly examined. In the end of each subchapter the major obstacles that influenced the project are highlighted.

4.1 Concept system to cure overflow

After analyzing the data relative to the LOCA which overflows the dam line hence infiltrates to the inside of the display, a concept was created for an Overflow Cure System.

It consists in curing the overflow right after assembly, before it gets into the cure station which is the next step in the production line. This way, it won't interfere with the spreading of the material dispensed in the active area while curing it in the shortest time possible. For this purpose, hot air convection is directly applied to the outside of the product, specifically where the LOCA overflows to the inside of the display.

Based on the temperature profiles analyzed, an increasing cure temperature triggers a faster start of the cure reaction exponentially, as one can see in Figures 7 and 8. Once the cure reaction starts, it cannot be stopped, hence, once the cure starts it is much likely that the material that eventually overflows stops spreading before it can reach the areas sensitive to infiltrations, due to increase of viscosity.

To materialize the system, the idea is to dispense heated air through air curtains oriented to the gap between display and glass, where the LOCA may overflow. Also, the temperatures to

be tested are higher than the temperatures shown in the previous data, in order to achieve shorter times of cure start, and also faster cure. Since the cycle time of the process is 3 minutes and this represents a short time period to expect the adhesive to cure, the times of exposure to the OCS will be multiples of the cycle time, between 3 and 9 minutes. Nevertheless, the temperatures to be tested will comprise a range of temperatures from 90 °C to 100 °C. It may seem as high overshoot in relation to the heat profiles previously used, but since the exposure will be shorter than it is during the process, this is explained as an incremental coefficient for satisfactory results tests. In spite of the analysis, this heat transfer method hasn't been tested on the process, so it may have flaws or be inconclusive of LOCA cure. Nonetheless, although it may be inconclusive, it may also be the first step towards innovation, providing solution to problems of the same nature.

4.2 Overflow Cure System

The overflow cure system (OCS) intends to stop the overflow of LOCA from going into the sensitive areas of the display by curing this material before it happens. This is achieved with hot air convection, focused in the affected areas. The major concern is that the system works not letting LOCA reach the insulation tape of the display, without occurring delamination or any kind of damage in the product.

Thus, after analyzing the data relative to the cure profile of the LOCA, a first concept system was created: apply hot air convection to the overflow sensitive areas of the product. Therefore, the prototype system mplyish the effect was projected having as major concerns the

The primary requisites to conceive the pneumatic system are displayed ahead:

- Pneumatic grid: available on site;
- Directional valves: several options available in stock;
- Precision flow regulator valves: not available in stock;
- Standard pneumatic tubing: several options available;
- Standard pneumatic fittings: several options available;
- Pneumatic air heater: not available in stock;
- High temperature pneumatic fittings (service temperature: 100°C): Not available in the plant;

- High temperature pneumatic tubing: not available in the plant;
- Pneumatic air curtain or nozzles: not available in the plant.

As a consequence of not having all the material required, national and international market research was done so that the needs were met, having special attention to components available in Bosch suppliers.

4.3 Components selection and Benchmarking

The major goal of the system is to heat air and then drive it toward the areas sensitive to LOCA overflow. Pneumatically speaking, the air needs to be controlled in terms of pressure, flow rate and quality. Therefore, the air that will feed the system needs to pass through an FRL (Filter Regulator Lubricator) unit, in order to filter, lubricate and set the pressure of the air, and afterwards a flow regulation valve assembled in-line. The components picked for this matter are Festo MSB4 comprising on-off valve, membrane dryer, pressure regulator valve, directional valve 3-2 and soft start valve, and one precision flow regulator valve for unidirectional flows with pneumatic connections G1/8 from Festo GRP series. The air feeding these components is at ambient temperature, thus they are connected with standard PUN tubing of 8 mm diameter. The heating element of the system is Leister's LE3000 (Attachment A – 1), with capability to adjust temperature through a potentiometer from 0 to 650 °C. The air curtains used to dispense heated air are Meech's 450 mm long Pneumatic Neublade Airstrip (Attachment A – 5). Since the service temperatures of this part of the system are higher (over 95°C) the material requirement of the pneumatic connections from heating element until the dispensing elements is a service temperature higher than the maximum temperature used in the system. There is some offer in the pneumatic industry for polymeric flexible which stands high temperatures, over 150°C but only for small pressure applications (below 2 bar in most of the cases). Thus, the component selected for these pneumatic connections is copper tubing of 12mm diameter, 1mm thickness since it can work with service temperatures higher than the maximum capacity of the heating element (650°C). This choice ensures more safety handling of the system.

The whole system is designed to assemble in an aluminum structure. The section of the aluminum profiles used in the structure is 45x45 mm from Rexroth standard series. These profiles are connected either by the screwed end in the center of the top and bottom sections or resorting to 90 degrees corners compatible with these profiles.

Regarding the insulation type, the lead property of the material is having low thermal conductivity, in order to have a minimum overshoot temperature set in the heater to achieve a constant temperature 75 to 95 °C in the air curtains outflow. For this matter, several insulations available in the market have been analyzed so that one could find the more viable option for the application. In terms of thermal conductivity, the mean values for the thermal conductivity as function of shrinkage shouldn't be very low (around 0,1 W/m.K), since copper tubing has high thermal conductivity (around 400 W/(m.k)). On the other hand, the thickness of the insulator shouldn't be higher than 20 mm, due to the tight space available between tubing and base structure. Between the most common materials for thermal insulations such as rock wool and glass fiber, the most appealing for this application is Pyrogel XT-E. This silica based aerogel has low thermal conductivity range from 0,02 to 0,09 W/(m.k) for a range of temperature comprising 0 and 600 °C, and non the less is available in 5 mm thickness rolls (Attachment A - 2). Although it represents a great match to insulate the system, this material isn't available in the local market, and for questions of time it was not possible to order this material. The alternative solution has been found with a material with very similar thermal properties from Superwool series of Morgan Thermal Ceramics (Attachment A - 3). This material is available in a wide range of density and thickness (Attachment A - 4). Finally, Superwool of 128 kg/m³ confers insulation with a thermal conductivity of 0,05 to 0,12 W/(m.k) for the same temperature range as Pyrogel XT-E, with a thickness of 6 mm. As mean of comparison, a calculation of the heat loss according to ASTM C680, issue 2004 for a plane surface with coating thicknesses of 6 mm and 13 mm of Superwool 128 kg/m³ with ambient temperatures of 450 and 20 °C for the inside and outside surfaces respectively. The Attachments A - 8 and A - 9 show the temperature transition along the insulation layer of 13mm. The profile gets colder as it gets near the outer wall. Now, the most important factors to evaluate are heat storage and heat loss, since the main reason for applying the insulation is to reduce the heat losses along the system. The worst case scenario is the tube connected to the heater's output, which will be exposed to the higher temperature in the system. The overshoot temperature of 450°C represents a safety coefficient in order to increase thermal efficiency of the system. The total heat storage in these conditions has a total value of 432.3 kJ/m², being that the heat loss has a total value of 1672.1 W/m². In the Attachments A - 10 and A - 11 one can observe the same profile analysis for the same working conditions, this time for a coating of 6 mm thickness. The results show a total heat storage of 345.4 kJ/m² and a total heat loss of 2673.1 W/m². As it seems, the double layer (13 mm thickness) insulation reduces heat loss in approximately 38%, in relation to the heat loss for single layer (6 mm) insulation, which is expectable as the thickness of the insulation layer

is more than twice bigger. As it goes for heat storage, the system insulated with single layer insulation holds around 20% less energy than the one with double layer insulation.

Therefore, the first version of the system was projected resorting to the components selected above and listed in the Bill of Materials shown in Table 11.

Table 11 – List of components

Component	Quantity	Description
Festo MSB4	1	RFL Unit + directional valve w/ soft start
Festo GRP G1/8	1	Precision flow regulator valve
Festo PUN 8mm tubing	1	Polyerethan pneumatic tubing
Rexroth Profile 45x45	7	Aluminum standard profile 45x45
Rexroth corner 45x45	4	profile 45x45 fixing corner
Leister LE3000	1	Air heater
Meech Neublade Airstrip	2	Pneumatic curtains
Aluminum Nozzle	1	Aluminum nozzle for air heater with G1/4 BSP
Racor G1/4 BSP – 12mm	3	Temperature resistant racor G1/4 BSP – 12mm
Racor “T” 12mm – 12mm	1	Temperature resistant racor “T” 12mm – 12mm
Racor 90° 12mm – 12mm	4	Temperature resistant racor “T” 12mm – 12mm
Aluminum curtain support	2	Aluminum L profile to support curtains
Workpiece support pillars	4	Workpiece support pillars
M10 screws	4	M10 screws to fix on top of 45x45 profile
M8 screws	12	M8 screws to fix on 45x45 profile channel
M5 screws	8	M5 screws
Thermocouple	1	Thermocouple

Superwool aluminum coated	1	Superwool 128 kg/m³ 6 mm aluminum coated
Copper tubing 12x1x5000		Copper tubing 12x1x5000

4.4 Assembly and setup

The sequency of assembly of the components described in the previous subchapter is available in the exploded views of the Attachment B, as well as the bill of materials.

Regardless, the first time the system was turned on until the last working prototype was complete several adaptations and changes were done over the initial project. The first assembly of the system as well as its later versions is described in this section.

4.4.1 OCS version 1

The technical drawing of the whole structure is also available in Attachment B.

In regards to the assembly of this system, the first group of components to be mounted is the base structure in 45x45 aluminum profiles connected with the steel brackets 45x45 or 90x45. The 3D model of the base structure is shown in Figure 22.

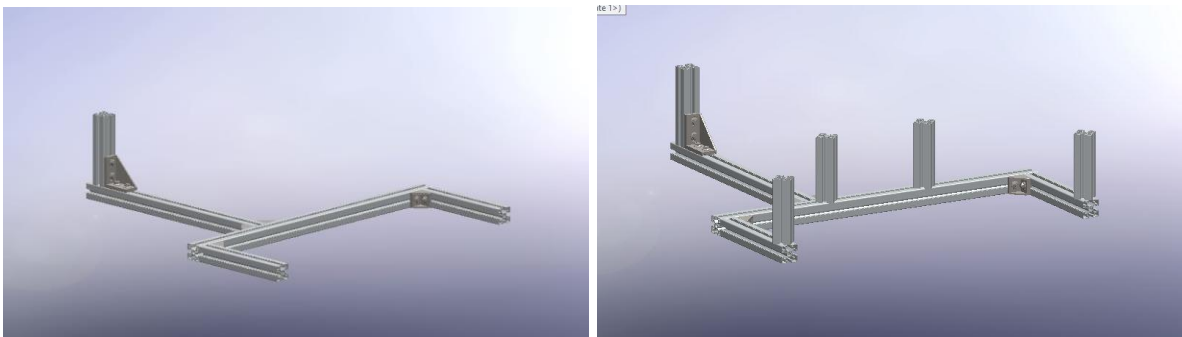


Figure 22 – Base structure with standard aluminum profiles (left); Base structure with support pillars for air curtains (right)

Afterwards the heater group of components must be previously assembled and then fixed to the structure with two M4 screws and nuts in the vertical profile in the back of the “fork” structure. The heater group is shown on the left side of Figure 23.

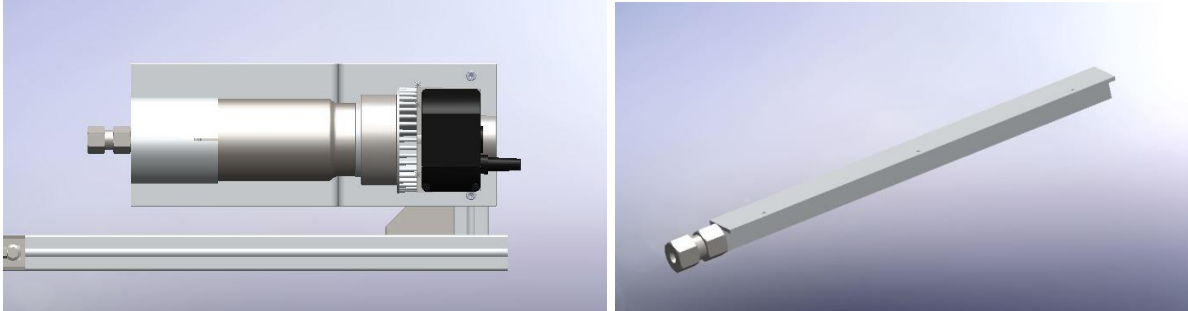


Figure 23 – Heater group fixed in base structure (left); Air curtains connected to a Racor ¼ G/12mm (right)

From this point, the next components to be mounted are the air curtains supports and the air curtains. The supports are fixed to the vertical profiles in front of the “fork” structure with M5 screws and hammer nuts, furthermore the curtains are fixed in the supports with three M3 screws and nuts. The position and angle of this components are adjusted when the whole structure is assembled. The fixation of these components is represented in Figure 24.

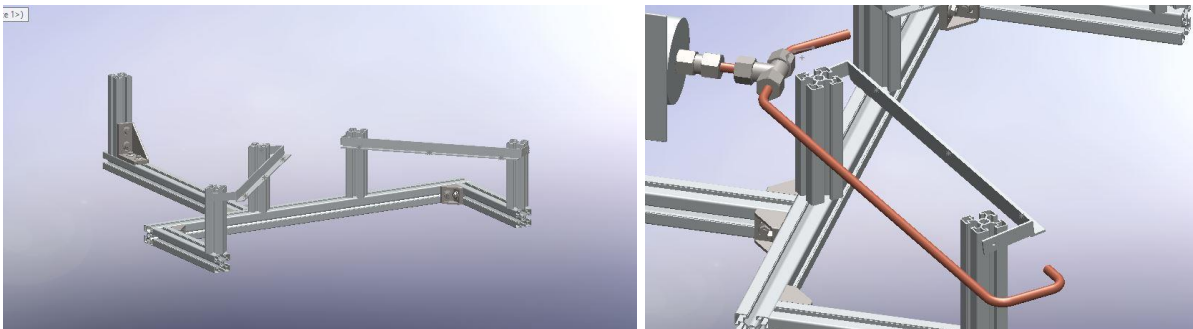


Figure 24 – Air curtains supports fixed to the base structure (left); piping installed in the heater nozzle (right)

After this point the racors and copper tubing are mounted connecting the heating group to the curtains. In the end of this action the system must be adjusted to give air flow in the required areas and respecting the previously stated requirements, using a sample workpiece to assure the positioning. The complete 3D model is shown in Figure 25 in the next page.

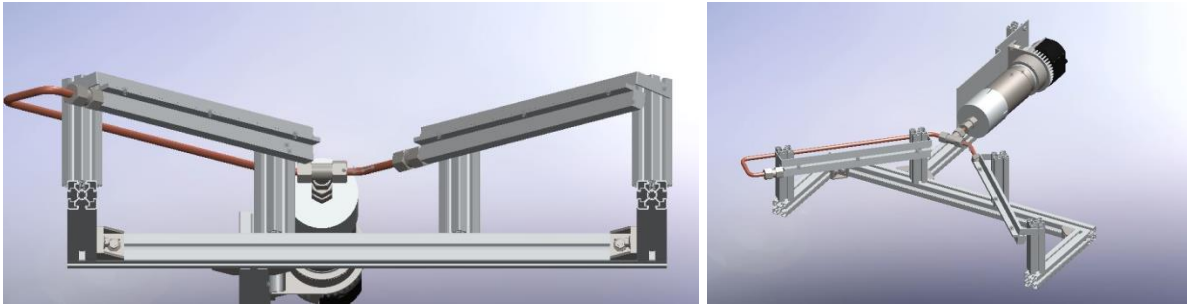


Figure 25 – Air curtains installed in the piping and fixed to the air curtains supports (left); Isometric view of the system (right)

Important to note that the angle of the air curtains support with the support pillars is slightly more than 90° and must be adjusted to the position of the workpiece, targeting the glass layer from below.

In the Figure 26 the real prototype of the system is shown, without and with insulation.

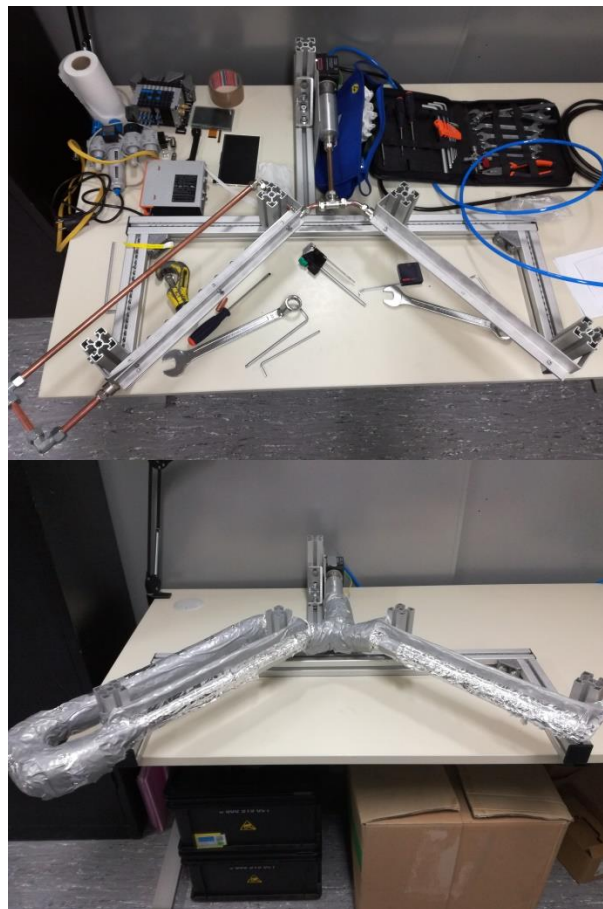


Figure 26 – Real system without insulation (up); Real system complet (down)

Although the system is designed to have a good and stable performance in terms of temperature and air flow, it is possible that it needs to be adapted or modified if the desired performance is not achieved, as referred in Figure 3 of the Project's Methodology section.

Furthermore, the test and analysis of the system is described in the next subchapter, along with the description of how the system is optimized focusing on the information delivered by the analysis.

4.4.2 OCS version 2

After assembling the whole system, it was put to run in continuous in order to assess if it was capable to stabilize in the maximum temperature of 95°C required for the tests. To do so, the system was instrumented with termopairs in the heater nozzle, three points along one air curtain and 2 points in the other, assuming that if the temperature is coincident in the first and last point of both curtains, the middle point will give information about the temperature distribution on both sides. In order to collect and transfer the data one used a thermoprofiler Mole with 6 channels and termopairs type K. Within Figure 27 one can observe the instrumented system with a zoom to the termopair placed in the heater nozzle.



Figure 27 – Instrumented system (left); Termopair in heater nozzle (right)

The instrumentation was designed to provide data relative to the temperature distribution in the system, namely during the early phase when the system is heating at different rates. This way its possible to identify if there is an undesired temperature diferencial between different components or parts of the components. Moreover, Figure 28 displays the instrumentation in the air curtains.



Figure 28 – Two termopairs in left air curtain (left); Three termopairs in right air curtain (right)

In a first analysis the system was running for one hour with the potentiometer in the level 2. The nomenclature used is shown below and also in Figure 29 along with the results of the thermal analysis:

- A – 1: Termopair in first point of right side air curtain;
- A – 2: Termopair in heater nozzle;
- A – 3: Termopair in middle point of right side air curtain;
- A – 4: Termopair in last point of right side air curtain;
- A – 5: Termopair in first point of left side air curtain;
- A – 6: Termopair in last point of left side air curtain;

The first conclusion is that the safety relay of the heater is shutting down the power without letting the temperature stabilize in the desired operating conditions. Also one can observe that the differential of temperature between the first and last point of the air curtains dispensing output is approximately 40°C and on the air curtain of the right side, in the middle point termopair the temperature is approximately 100°C. Combining this information with the length of 450 mm of the air blade dispensed in each curtain, one can state that there is a linear decay of temperature in these aluminum components of around 8,9°C/100mm. Moreover that is some noise in the data recovered from the termopairs in the first point of the air curtain in the right side, which can be explained by being the point exposed to more turbulent air flow due to being connected with the shortest length of pipe in the system. This statement is also supporting by the fast heating, being the second point that heats and cools faster after the point in the heater nozzle which is the source of heat.

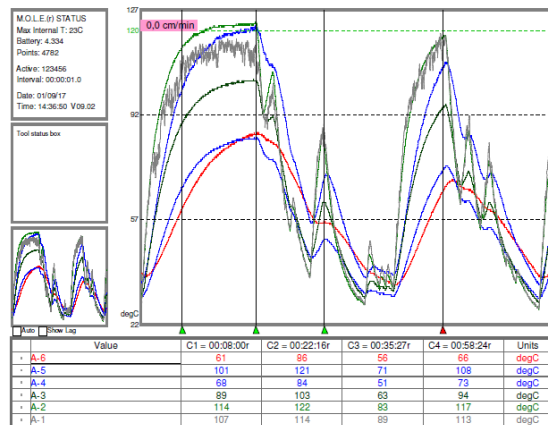


Figure 29 - Termopile of OCS version 1 with potentiometer of heater set in level 2 scheme of instrumentation
 The same test was conducted for the 6 level of the potentiometer which represents maximum power of the heater, working continuously for around 30 mins to access if the problem persists. The result is shown in Figure 30 and its nomenclature is:

- A – 1: Termopair in heater nozzle;
- A – 2: Termopair in first point of right side air curtain;
- A – 3: Termopair in middle point of right side air curtain;
- A – 4: Termopair in last point of right side air curtain;
- A – 5: Termopair in first point of left side air curtain;
- A – 6: Termopair in last point of left side air curtain;

The profiles reveal a decay of temperature in the all points after it reaches a peak temperature of around 260 °C. Concerning the temperature differential on the air curtains, the three points analysis shows, once again, a linear decay. Although the temperature loss is similar, with this greater feeding temperature the differential between the first and last points of the air curtains is now of around 70°C, which suggests the higher is the feeding temperature the higher will be temperature differential in these components. In comparison to the previous test the linear decay of temperature is 15,6°C/100mm which is approximately the double as in the previous attempt.

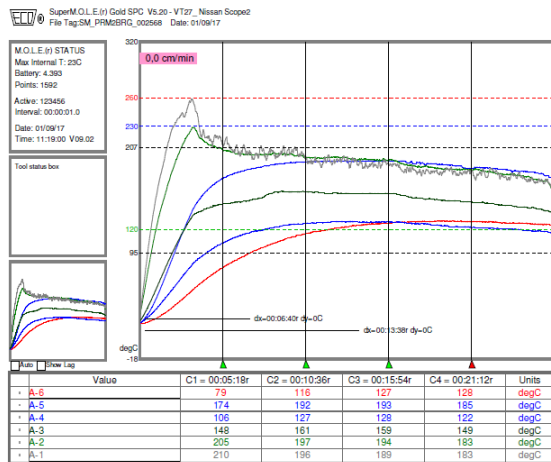


Figure 30 - Thermoprofile of OCS version 1 with potentiometer of heater set in level 6 scheme of instrumentation

In order to achieve the desired function on the system the next upgrade was to replace the aluminum air curtains with an alternative solution. Another problem of the current set up was that the heater was not able to keep the temperature stable in a high level, and combining this information with the temperature loss in the air curtains one possible explanation is that this components are absorbing too much heating hence overloading the heat source without achieving the desired temperature in the output.

The solution found passed through making a symmetric pipe path aiming at the two corners of the display that are critically affected by the overflow of uncured OB.

After some attempts the new model created consists on the shape shown in the Figure 31 in the next page, where both outputs are solely constituted by the same copper pipe used to connect the heater to the air curtains, pointing at the exact point where these corners of the display will be positioned during the experiment.

The air is dispensed upstream beneath the glass which allows the air to spread all over the area in the corners between the display and the glass and hence trigger the cure effect more effectively.

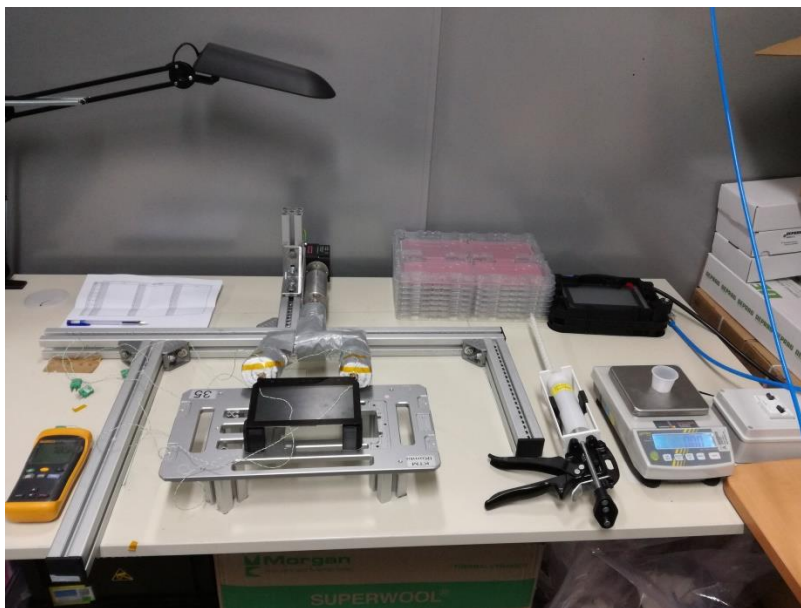


Figure 31 - OCS version 2

In this simplified version of the system the temperature control was made resorting to a different kind of monitoring. This time the evaluation resorts to one termopair in each output and one termopair in each of the affected corners of the display.

The goal of this evaluation is to check if the system is stable in the output and in the targeted areas, also to check the real temperature of the air in when it reaches the display surface, between display and glass where the OB is meant to be cured. This instrumentation can be observed in Figure 32.

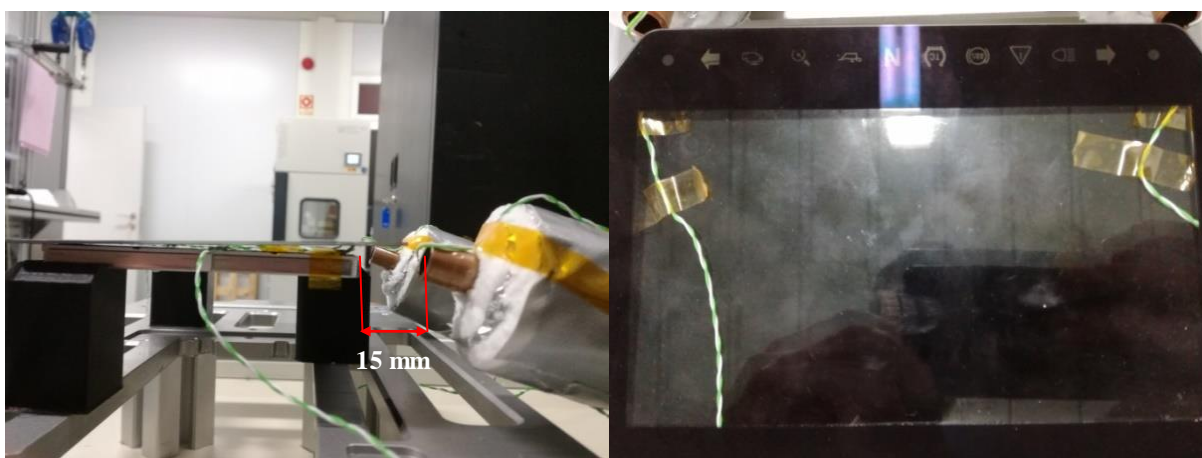


Figure 32 – OCS version 2 instrumented (left); termopairs in the affected corners of display (right)

Due to unavailability of Mole Termoprofiler for this analysis, the hardware used was four units of Fluke 51 II Thermometer to monitor the four instrumented points and the results are shown in Figure 33 for a period of around 15 mins.

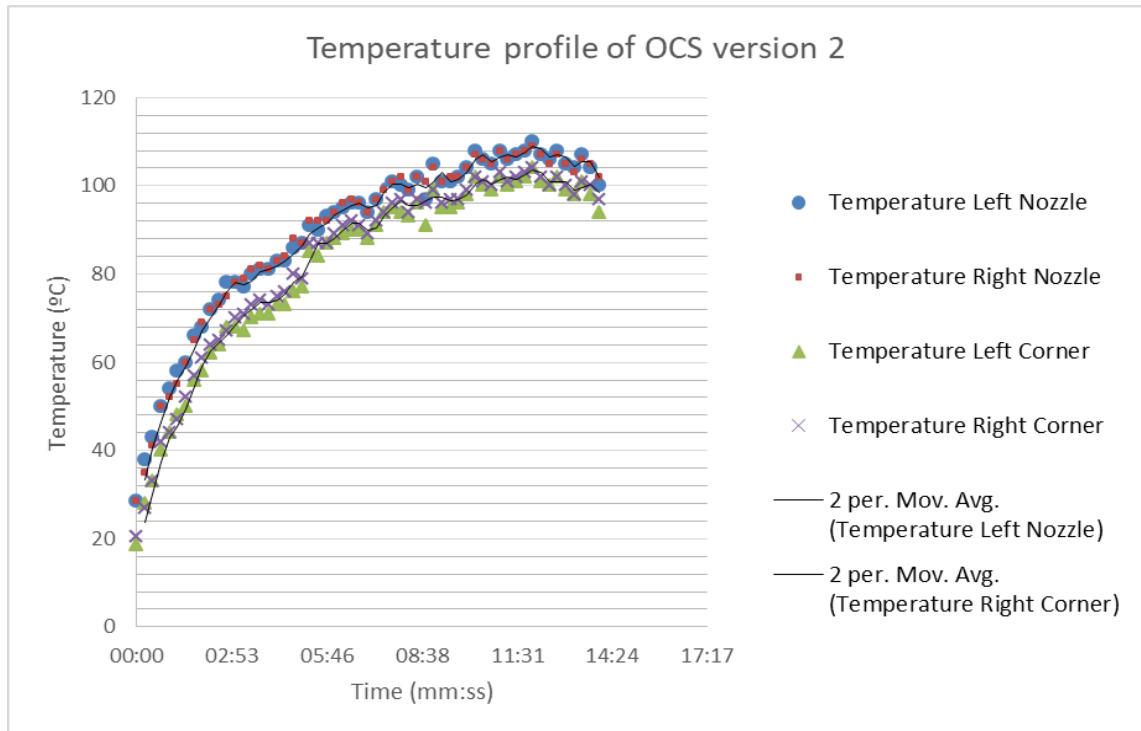


Figure 33 - Analysis of OCS version 2 with working continuously for a 15 min period with heater set to 5

The information provided by the analysis proved that the upgrades of the system overcame the goal of stabilizing in a temperature, in this case within a range of ± 3 °C around a reference temperature below 105 °C. Both tendencies lines in the dispersion of the nozzle and corners of the display show that the system is heating and stabilizing at the same pace for both right and left sides. Moreover one can state that the temperature distribution in the corners of the display oscillates around a value 6,5 °C lower than the instant temperature of the air flowing out of the nozzles.

Afterwards a second evaluation was performed, although this time the goal is to get the complete temperature profile of the system. In order to control the temperature, the system is now instrumented only in the corners of the display, since the temperature differential between nozzles and corners of display was concluded to be approximately constant after the heating stage. This way the temperature monitored is the test temperature. In detail, the system is now controlled respecting the following steps:

1. Start the system setting the potentiometer of the heater and overshoot the temperature above 100 °C in order to assure that electrical hysteresis won't affect the performance;
2. Slightly reduce the power in the potentiometer of the heater until the reference temperature read in the thermopairs is 95 °C;
3. Slightly reduce the power in the potentiometer of the heater until the reference temperature read in the thermopairs is 85 °C;

4. Slightly reduce the power in the potentiometer of the heater until the reference temperature read in the termopairs is 75 °C;

This stages represent the heating stage and the stabilization of the system for the temperatures to be tested. In each of the stages after the first when the system is put to run must keep the temperature steady for at least 9 mins so that it is possible to assess whether the system is capable of performing the longer tests keeping the temperature stable within a minimum error.

Finally the results for this analysis are shown in Figure 34, where the four stages can be observed among the transition phases. The thermo profile reveals a heating stage similar to the previous analysis, although the maximum overshoot temperature is slightly lower than the peak temperature shown in Figure 33. After this early stage, the temperature lowered to the tests temperature as expected. Also the minimum time that the instrumented display was exposed to the test temperatures has been achieved, being that during the the stage in 85°C the left corner achieved the desired temperature quickly than the right side and there in one value that falls out the dispersion in first two minutes of this stage. Nevertheless most of the values read in the steady stages 2, 3 and 4 are consistent keeping the dispersion with a constant range of values.

Regarding the behavior of the profile during the transition phases, it was measured that the time needed to cool the temperature by 10 °C in the corners of the display is around 2 mins, for the temperatures tested.

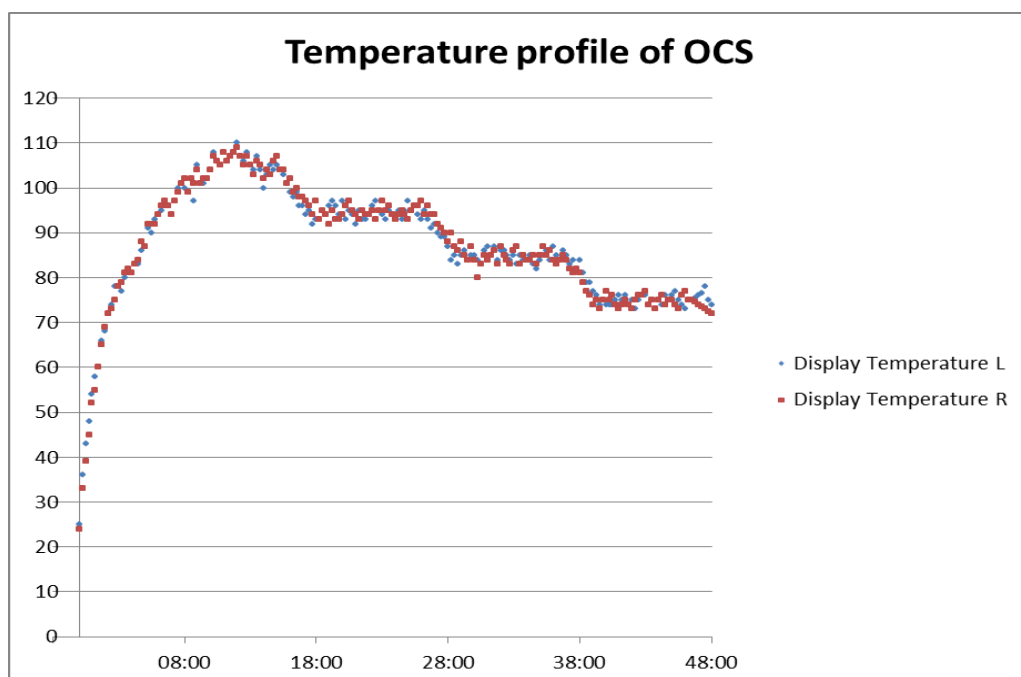


Figure 34 - Temperature profile of OCS monitoring temperature in the corners of display

Last but not the least, the system must be operated within the factors acknowledged in the profile. Resorting to Figure 33, a heating period of around 8 min is proven to be enough time to achieve 100°C. As a safety coefficient the heating period is characterized as 15 mins, after which one can control reduce the power in the heater until the desired temperature is achieved as shown in Figure 34

Compiling the data extracted from this temperature profiles, it was defined that when the machine is put to run from ambient temperature it must operate continuously for 15 mins with the heater set to level 5, overshooting the temperature of 100 °C. After this period the potentiometer of the heater should be adjusted until the temperature in the corners of the instrumented display is reaches the test temperature (in this case [75; 85; 95] °C). It's critical to execute the previous steps respecting the position of the display in the base structure, assuring position hence performing a valid temperature measurement. Concerning the transition phases, for the same reason of assuring that the temperature is completely stabilized by the moment of the test it was suggested to wait 3 minutes and perform a new evaluation of temperature with the instrumented display when the system's temperature is being changed by 10°C down. For a matter of simplicity handling the system during the experiment another requirement is to overshoot the desired temperature and then adjust it by lowering the power in the heater potentiometer, which corresponds to the known thermic profile of the system.

4.5 Supports for product during experiment

One key component of the experiment is the work piece supports, which need to ensure precise positioning product's components from the second station, first in the laboratorial setup, until the last when the LOCA is fully cured.

In the tests, the assembly the display and glass layers is performed with a manual assembly jig, consisting in performing the movement of the cover layer over the display layer previously fixed in the work piece supports as explained in Chapter 3. During testing in the OCS station, the product is placed 55 mm from the bottom of the structure, so that the air nozzles can target the affected areas of the product from bellow ensuring that the air won't be blocked by the margins of the glass that are not covered by the display after assembly. Thus, custom parts were designed and are presented in this chapter. In summary the target of these supports is to ensure the position of the display in the center of the bottom layer of the jig with a height of 55 mm, which gives enough space for the nozzles to be placed close enough

to the display and produce the desired effect without interference of the kit and the glass layer. The 3D model of the supports previously described in this section are displayed in Figure 35.

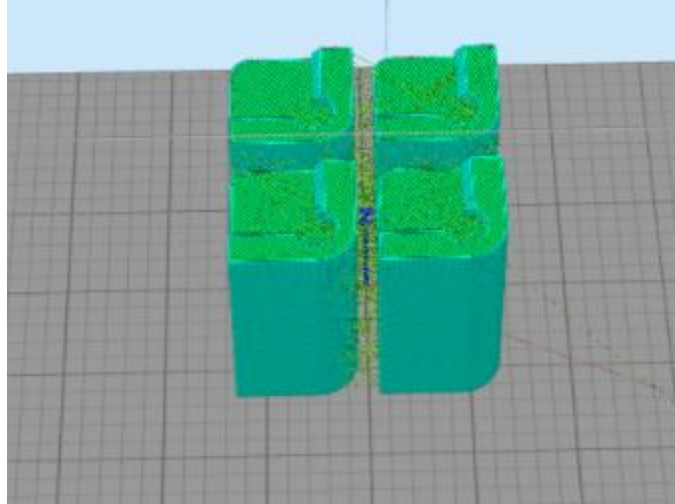


Figure 35 – 3D model of product supports comprising four corner pillars

Each support has three orthogonal surfaces to ensure the display tightly positioned at the desired height in the center of the manual jig. These components were made in a single production (four units only), and needed to be produced as quick and economically as possible, respecting a good surface finish. The process chose to make the physical model was additive manufacturing. Although this technology is quite recent, in the last years it revealed to be a great asset in the rapid prototyping (RP) panorama, making it a powerful tool in terms of reducing development time in assemblies, product testing or tooling for short or medium run production [24].

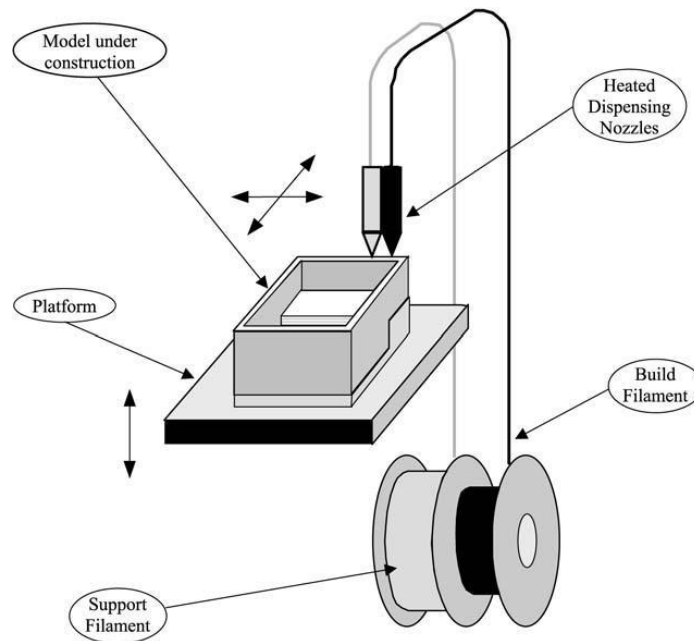


Figure 36 - Schematic of the FDM process

In detail, the technology used to produce the support pillars was fused deposition modeling (FDM) which is represented in Figure 36, and almost half of the machines which were introduced to the market belong to this category. Therefore, a filament of material is extruded out of a fine nozzle and deposited onto a platform. The nozzle moves in the X-Y plane so that the filament is laid down to form a thin cross-sectional layer of the part. The platform is then lowered relative to the nozzle and the next layer of the part is deposited on top of the previous layer. As the extruded filament is hot, it bonds to the material in the previous layer. A second nozzle is used to extrude another filament, in order to include a different material composition in the part or build-up support structures for the part where needed. Once the part is completed the support structures must be broken away from the part. The materials applied in FDM are ABS, elastomer, investment casting wax and polycarbonate [25]. The main parameters that control the process are layer thickness, road width and speed, but nevertheless, temperature, humidity and wire diameter must be controlled as well. [24].

Finally, it was decided to produce the support pillars in 3Dadd FDM machine, as they proved to have a finely controlled process where a good quality/price ratio is expected, relative to the national panorama. The process parameters were customized for this application.

The tool parameters were set to only use one nozzle of 0,40 mm diameter with a speed of 2000 mm/min, as shown in Figure 37.

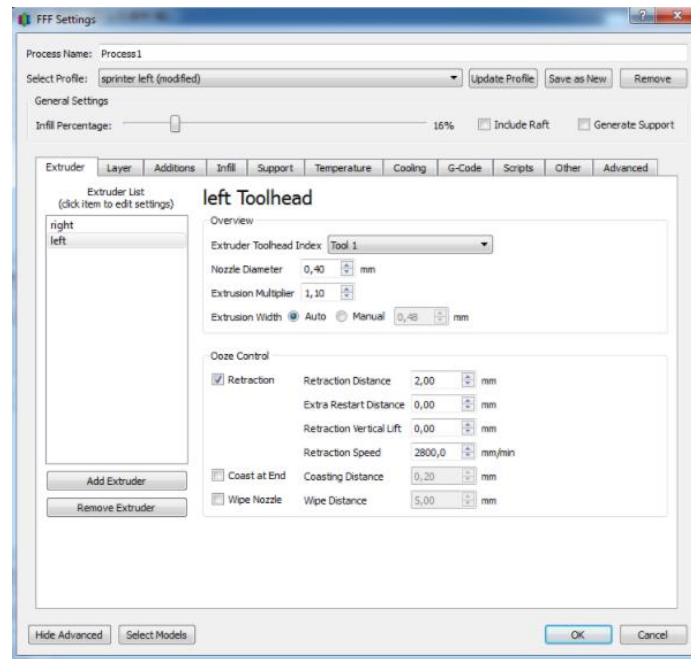


Figure 37 – FDM machine tool settings

For the layer deposition control, two different features were controlled. The outline of the body, comprising bottom layer, top layer and perimeter shell, that was made with solid composition so it would ensure dimensional requisites and fine surface finish, and the infill.

As shown in Figure 38, the parameters were 0,20 mm height, inside-out direction, and 80%, 130% and 50% for first layer height, width and speed respectively.

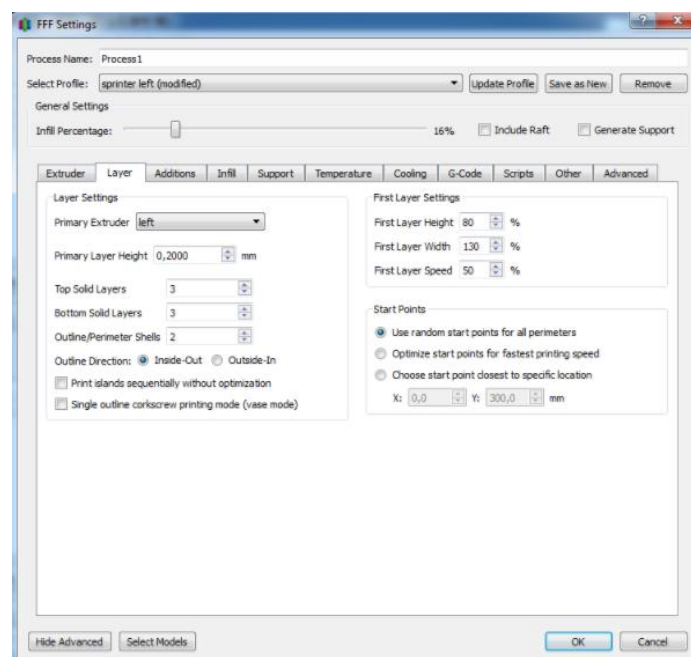


Figure 38 – Layer settings on FDM machine

On the other hand, the interior of the layers, named infill, was set to have a faster deposition and hence less dense composition. This method allows faster prototyping, less product weight and raw material saving, furthermore lowering the price for the production run. The settings for this feature are shown in Figure 39. The interior fill percentage was 16%, as its extrusion width was 100% and the orientation of these layers is an array turned 45° in relation to the outline layers.

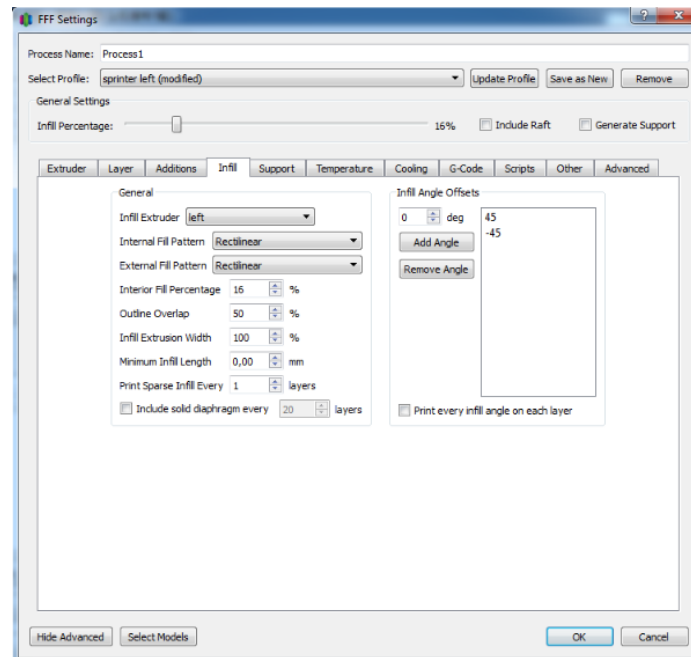


Figure 39 – Infill settings on FDM machine

The deposition of the infill layers can be observed in Figure 40 in the next page, where low density core is deposited within the outline solid layers.

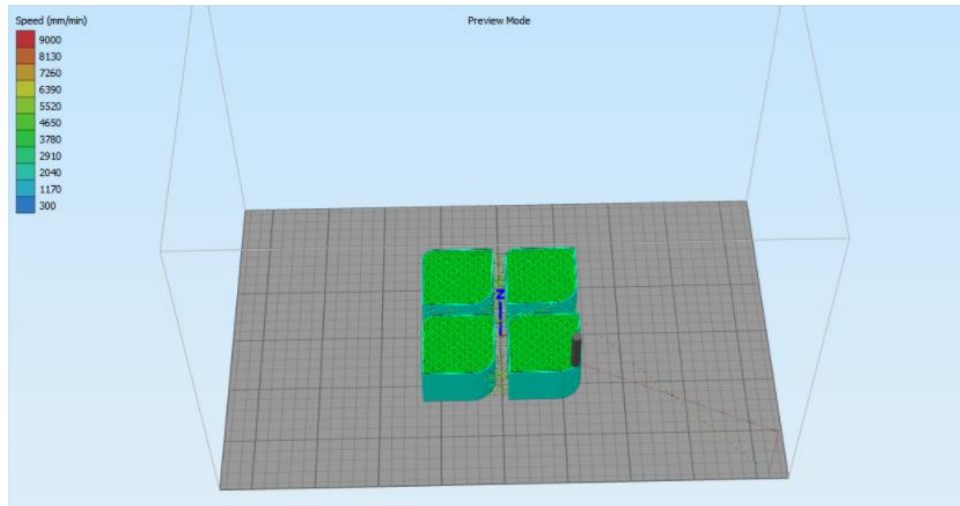


Figure 40 – Representation of infill layers

The results are satisfactory in all three surfaces that contact with the product in terms of surface finish and capability to fix the product in the desired position.

5. Experimental data analysis

The results are shown in this chapter along with the respective analysis, in regards to the testing of the OCS in the Optical Bonding process as a means to tackle the problem due to LOCA overflow.

The focus is to identify if either there is a test parameterization that provides an efficient solution for the problem, or a tendency that may provide useful data for the future work.

Moreover the analysis comprises evaluation of results, description of results, statistical analysis and finally discussion about the effects or tendencies that have significance in the experiment.

In the end there is a subchapter dedicated to describe the implementation of the system, adapted with the inputs that the experimental data provides.



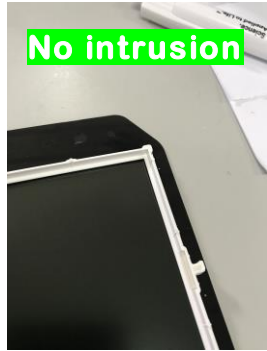




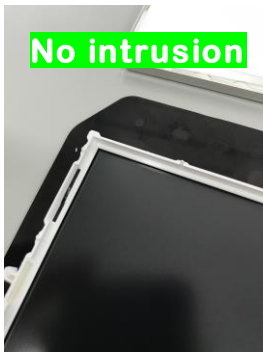




5.1 Results description and DOE analysis

In the early part of this chapter shows the observations to the experimental work that have to be kept in mind when analyzing the results. In general, no problems happened concerning the execution of the experiment. However, the tests 11, 12 and 13 according to Table 5, are not valid because the amount of LOCA dispensed was lower than the minimum amount defined for the process. The mistake was found by the end of the test 13 when the measurement of the amount of LOCA remaining in the cup from which it is dispensed on the display was considerable, representing near 1 g of material. For this reason, the amount of LOCA that is effectively dispensed in the display during this step of the process is controlled with a scale. Therefore, one measures the total weight of the cup and adhesive and then dispense it on the display until the difference between initial weight and current weight of the cup and adhesive together is at least the same as the minimum amount of LOCA that the product requires,

rather than dispensing the right amount of it that must be dispensed on the display inside the cup.

Furthermore the criteria of evaluation is described in Table 12.

Table 12 – Description of the measurement in the response

Class	Tape	Corners	
0			
1			
2			
3			

In order to compare the results, the response of the experiment is a numeric classification where 0 represents the best result without intrusion of LOCA and with the insulation tape dry, and 3 represents the worst outcome of having intrusion in both corners that are usually affected by this problem along with the insulation tape wet with LOCA. The method of evaluation passes through a destructive process of the frame of the display, in order to observe the interior zones, evaluating the state of the insulation tape and the corners of the active area.

To do so it is necessary to cut the stakes that fix the outer frame to the inner structure (heat staking), afterwards take the top layers of the display until it is possible to see the tape with no obstruction. The results are shown in Table 13.

Table 13 – Results of overflow cure experiment

Test	Class	Description
11	0	No intrusion in both corners
12	0.5	Intrusion in one of the corners
13	0	No intrusion in both corners
14	2	Tape wet in one of the sides
21	2	Tape wet in both sides
22	3	Intrusion in both sides
23	1.5	Tape wet in one of the sides
31	2.5	Slight infiltration in one of the sides
32	0	No intrusion in both corners
33	2.5	Slight infiltration in one of the sides
41	1.5	Tape wet in one of the sides
42	1.5	Tape wet in one of the sides
43	1.5	Tape wet in one of the sides
51	1.5	Tape wet in both sides
52	1.5	Tape wet in one of the sides
53	3	Tape wet in both sides
61	1.5	Tape wet in one of the sides
62	2	Tape wet in both sides
63	1.5	Tape wet in one of the sides
71	0	No intrusion in both corners
72	0	No intrusion in both corners
73	1.5	Tape slightly wet in one of the sides
81	1.5	Tape slightly wet in one of the sides

82	1.5	Tape slightly wet in one of the sides
83	1.5	Tape wet in one of the sides
91	0	No intrusion in both corners
92	0	No intrusion in both corners
93	0	No intrusion in both corners

The left column refers to the identification of each test, being that the first number corresponds to the parameterization set for the test shown in Table 4 of the DOE, after which follows the number of run, from 1 to 3. Thereafter there is an exception for test 14, which is an additional test, because none of the 3 repetitions with parameterization 1 was valid.

In order to better understand the results a 2D map was created to compare the results of each parameterization, which is shown in Table 14. According to the cure profiles of LOCA described in the state of the art, it is expected that the results are better as they get closer to the bottom and right sides (increasing temperature and time).

In the Table 14, the values shown are corresponding to the test results, and below, the average value of the three repetitions for each parameterization. The smallest number in the colored area corresponds to the parameterizations in Table 4.

Table 14 – 2D analysis of OCS tests

		Time (mm:ss)								
		03:00			06:00			09:00		
Temperature (°C)	75	2	-	-	1,5	1,5	1,5	0	0	1,5
		1	2		4	1,5		7	0,5	
	85	2	3	1,5	1,5	1,5	3	1,5	1,5	1,5
		2	2,17		5	2		8	1,5	
	95	2,5	0	2,5	1,5	2	1,5	0	0	0
		3	1,67		6	1,67		9	0	

In a first approach, when looking at the influence of each variable, it seems that for the tested range of time and temperature, time increase couples with better results. Nevertheless, the

best results are achieved for the parameterization of maximum time of exposure combined with maximum temperature. For this parameterization, the system is able to stop overflowing from reaching the sensitive areas of the display in all the three times repetition.

The tool used to validate and draw more accurate conclusions is the Factorial design analysis referred to in the state of the art. The statistical analysis used the software Minitab 18 and the graphic data and tables within this subchapter that are shown from this point on are exported from the same software.

The inputs of the factorial design are shown in Table 15 in the Design Summary and Factor Information. The factors are defined as Temp and Time standing for Temperature of the air in the targeted zones of the product and time of exposure of the product to the OCS respectively.

Table 15 - Design Summary and Factor Information
(from Minitab)

Factors:	2	Replicates:	3
Base runs:	9	Total runs:	27
Base blocks:	1	Total blocks:	1

Factor	Levels	Values
Temp	3	75; 85; 95
Time	3	3; 6; 9

In the analysis of the design the standard confidence interval used is 95%, being that the α -level is 0.05.

Focusing on the analysis the first stage comprises the main effect and interaction analysis, in order to understand which tendencies may have real importance for the work. Therefore these effects are validated in terms of statistical significance in order to assess if the observed tendencies have real meaning with statistical confidence.

The main effects for each factor were calculated and the plot is shown in Figure 41. Observing this figure it is possible to say that factor Time as the greatest impact in results as its main effect significantly reduces the response to the targeted values. In detail from the point of 3 to 6 minutes the response decreases slightly, given that from 6 to 9 minutes it decreases very significantly lowering the average response from 1,75 to near 0,65.

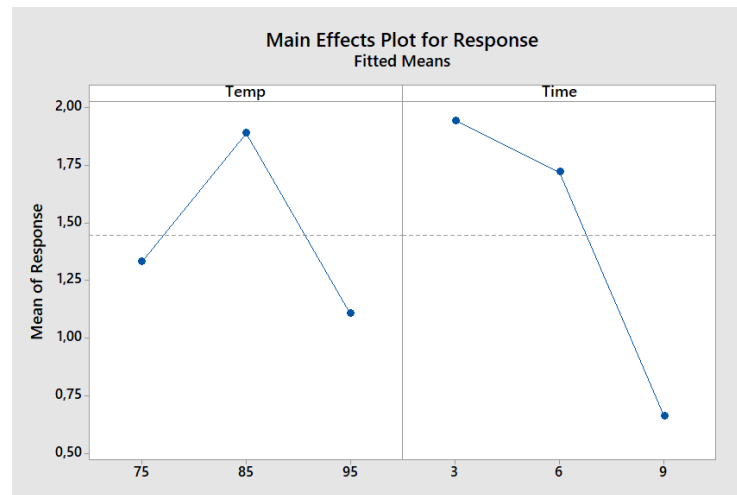


Figure 41 – Main effects plot for response

However, in the main effect plot of factor Temp, the variations of the average response do not match the expectations. It was expected to have decrease in response for higher temperatures. However, from the low to the middle level of this factor, 75°C to 85°C, one can observe an increase in the response until the peak average value of the response in terms of Temp, which rejects the hypothesis of having a better response with a temperature increase. Nevertheless from 85°C to 95°C the response decreases, reaching a slightly lower value than the average response for 75°C.

In order to deeper evaluate the effect of interaction between factors on the response, the average response of each factor was evaluated for all the levels of the other factor. The plot is shown in Figure 42.

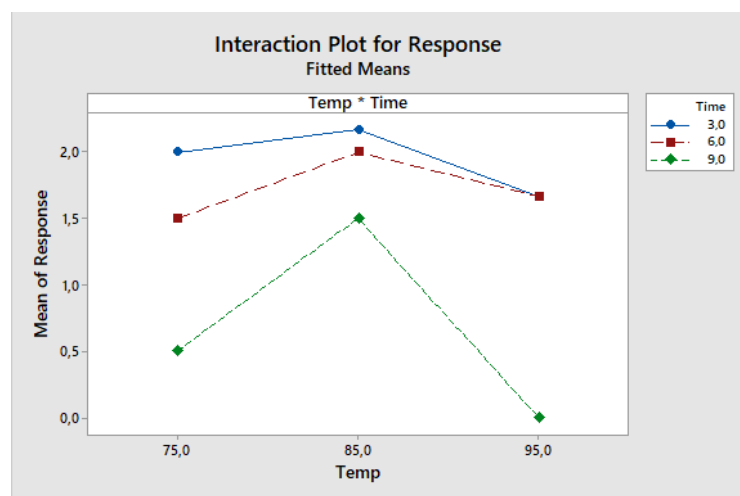


Figure 42 - Interaction plot for response

The graphic data suggests that there is small interaction Temp*Time except in the convergence of the lines of 3 and 6 minutes for a temperature of 95°C. The high level of the factor Time one represents the best results of the response in terms of Temperature. Regarding the Time*Temp plot there is slight interaction of the factors between the lines of 95°C and 75°C. Again there is the evidence that an increasing time plays an important role in decreasing the response, since this phenomena occurs for all the levels of the factor temperature.

The equation shown below is used to calculate the fitted values of the model for each parameterization of the DOE. Based on the comparison between the fitted values and the real values of the experimental work that are shown in Tables 13 and 14, the errors are calculated and displayed in Table 16 within the next page. The standardized residuals analyzed further in this chapter are based on this analysis.

$$\begin{aligned} \text{Response} = & 1,444 - 0,111 \text{Temp}_{75} + 0,444 \text{Temp}_{85} - 0,333 \text{Temp}_{95} + 0,500 \text{Time}_{3} \\ & + 0,278 \text{Time}_{6} - 0,778 \text{Time}_{9} + 0,167 \text{Temp*Time}_{75\ 3} - 0,111 \text{Temp*Time}_{75\ 6} \\ & - 0,056 \text{Temp*Time}_{75\ 9} - 0,222 \text{Temp*Time}_{85\ 3} - 0,167 \text{Temp*Time}_{85\ 6} \\ & + 0,389 \text{Temp*Time}_{85\ 9} + 0,056 \text{Temp*Time}_{95\ 3} + 0,278 \text{Temp*Time}_{95\ 6} \\ & - 0,333 \text{Temp*Time}_{95\ 9} \end{aligned}$$

From the Table 16 it is possible to observe that the greater error occurs in the second of the parameterization with 95 °C and 3 min, as well as the most frequent residual is 0 which occurs for 10 out of 25 valid tests.

Table 16 – Errors for each run of the DOE

Temp (°C)	Time (min)	Fits	1st Run	Error	2nd Run	Error	3rd Run	Error
75	3	2,00000	2	0,000	-	-	-	-
85	3	2,16667	2	-0,083	3	0,278	1,5	-0,444
95	3	1,66667	2,5	0,333	0	-0,833	2,5	0,333
75	6	1,50000	1,5	0,000	1,5	0,000	1,5	0,000
85	6	2,00000	1,5	-0,333	1,5	-0,333	3	0,667
95	6	1,66667	1,5	-0,111	2	0,167	1,5	-0,111
75	9	0,50000	0	-0,333	0	-0,333	1,5	0,667
85	9	1,50000	1,5	0,000	1,5	0,000	1,5	0,000
95	9	0,00000	0	0,000	0	0,000	0	0,000

The standard distance distance that the data values fall from the equation is measured by S in units of response. Thus, the S calculated in Minitab 18 for this model is 0,687184, value that indicates that the standard deviation of the data points around the fitted values is less 0.69. One can state that the model is adequate to the experimental data.

In order to compare the relative magnitude and the statistical significance of both main effects and interaction effects previously referred to, the p-values of the analysis of variance and the pareto chart of the standardized effects will be interpreted.

Focusing in the p-values of the Analysis of Variance shown in Table 17 it is necessary to compare these values with α -level. Given that the value of α -level previously defined is 0.05, a component of the DOE is validated with 95% of confidence if its p-value is lower than 0.05. Therefore it is only possible to validate the effect of factor Time with this confidence interval, since it is the only p-value among factors and interaction minor than 0.05.

Despite the previous interpretation, there is statistical meaning for the variable Temperature with a confidence interval of 90% for which the α -level is 0,1, given that p-value for this factor is $0,072 < 0,1$. Concerning the interaction, the p-value shows that there is poor significance in this effect with a reliable confidence interval.

Table 17 – Analysis of Variance (from Minitab)

Source	DF	Adj SS	Adj MS	F- Value	P- Value
Model	8	12.667	1.5833	3.35	0.016
Linear	4	11.278	2.8194	5.97	0.003
Temp	2	2.889	1.4444	3.06	0.072
Time	2	8.389	4.1944	8.88	0.002
2-Way Interactions	4	1.389	0.3472	0.74	0.580
Temp*Time	4	1.389	0.3472	0.74	0.580
Error	18	8,500	0.4722		
Total	26	21.167			

The graphic analysis shown in Figure 43 supports the previous statements. According to the figure, not only the greater standardized effect belongs to factor time, as well as it is the only one that passes the reference line (mean standardized effect), which means that only the effect of factor time has a statistically significant effect on the response. Although the standardized effect of Temperature is lower than the mean standardized effect, it is still very close to this value, which is an indicator that this factor has meaning for a lower confidence interval than the initial 95%.

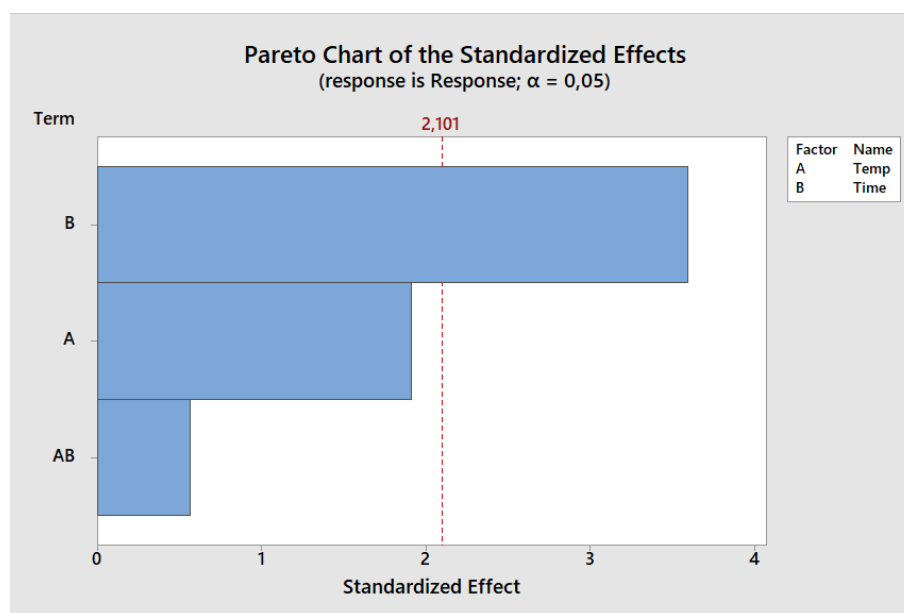


Figure 43 - Pareto chart of standardized effects

Therefore, the conclusions previously taken from effect of interactions are discarded for lack of statistical significance.

Although the model is evaluated in terms of variance and how well it fits the data, it still needs an analysis of the residuals.

The standardized residuals shown in Figure 44 in the next page for each factor are comprised in the interval between -2 and 2, which means that the residuals fit the regression with the confidence interval of 95%. Nevertheless the points marked in the plot with a red circle represent the test with the greater deviation from regression, with the standardized residual slightly above -2.

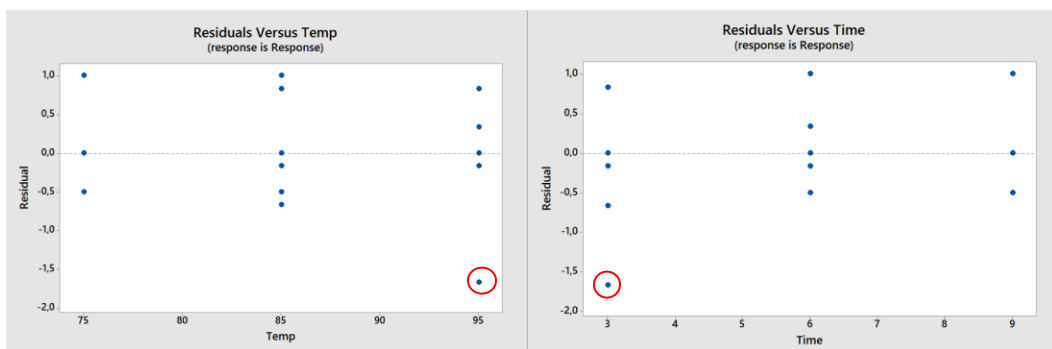


Figure 44 – Plot of residuals vs temp (left); Plot of residuals vs time (right)

Moreover a basic statistic analysis was done on the residuals data along with the Anderson - Darling Normality Test and it is summarized in Figure 45.

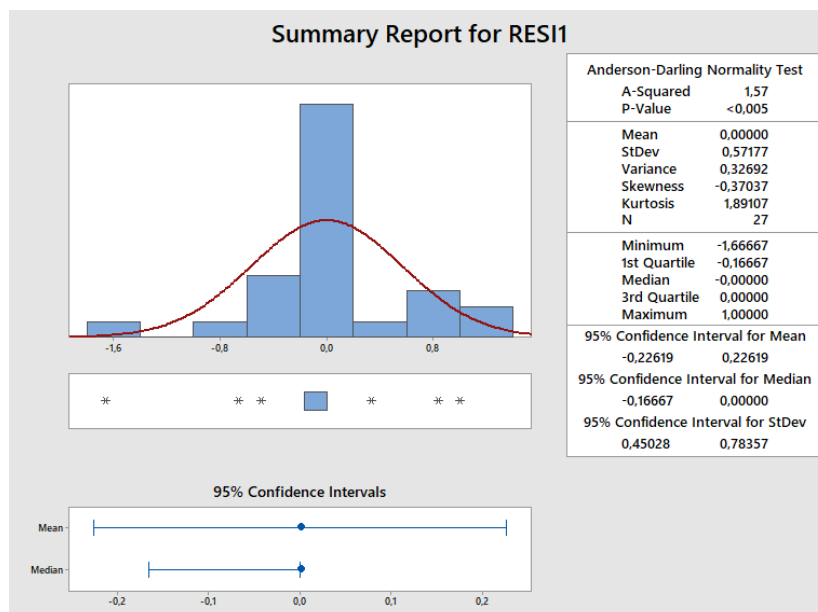


Figure 45 – Summary report of Anderson-Darling Test on the residuals data

The graphical data suggests that the residuals do not follow a normal distribution, as well as the p-value <0.005 rejecting this hypothesis. It is possible to conclude with a 95% confidence interval that the mean of the standardized residuals is between -0.22619 and 0.22619, also that its median is between -0.16667 and 0.00000, and that its standard deviation is comprised between 0.45028 and 0.78357. In the descriptive statistics of the residuals shown in Table 18 the mean values of these parameters are displayed.

Table 18 - Descriptive Statistics of the residuals (from Minitab)

Variable	N	Mean	SE Mean	StDev	Minimum	Median	Maximum
RESI1	27	0,000	0,110	0,572	-1,667	-0,000	1,000

The analysis concludes that time is the only significant factor present in this evaluation. The best results appear for the high level of this factor. This factor also has the greater modulus on main effect in this experiment, affecting around -1,25 in the average response from the low level to the high level. Although the analysis proves only the effect of the time factor, new tests should be done so that it is possible to test more levels of the factor temperature for a stage of 9 minutes with more repeatability, in order to get the results allow to draw significant conclusions about this factor and optimize the system. Nevertheless the test parameterization that overcame the problem that motivated the project is the combination of a 9 minutes stage with a temperature of 95°C. The exposure times of 3 and 6 minutes reveal an ineffective response to the problem, since either the tape is wet or there is intrusion of LOCA in the other tests. Having this in mind one concludes that the cycle time of this additional process is about 9 minutes, equivalent to three times the cycle time of the whole Optical Bonding process.

5.2 Implementation

The experimental data proves that the OCS is able to stop the problem of infiltration when set for 95 °C of temperature for a period of 9 minutes. Coupling this knowledge with knowing that the cycle time is 3 minutes, this step of the process becomes the bottleneck of the whole process. In order to overcome this obstacle the solution passes from having a station comprising three OCS. In another perspective there should be 3 overflow cure systems in

parallel within a short distance of the main line of transport, right after the area where the product leaves the assembly station. The Figure 46 illustrates schematically how the assembly of a triple overflow cure system looks like.



Figure 46 – Triple overflow cure system setup

Moreover, one linear conveyor (from line to station) and further a distribution conveyor (lateral movement along the three stations) transportation the product from the main transportation line to the respective station. The control of this conveyor is ruled by timed interactions between sensors and the motion system. This means that when one product finishes being assembled, one of the overflow cure systems must be vacant, so that the product is delivered in that vacant system. After the product stops and position is verified with sensors or vision software, the OCS turns on and triggers a timer which will turn it off 9 minutes later. On this moment the distribution conveyor receives the signal to pick it up to put it back in the main line. Every three minutes one piece of product leaves and another enters this station. The time necessary to fill the line from rest until its normal working conditions in 9 minutes, time necessary to perform 3 cycles.

Last but not the least, the whole system is modular because it is built in the same aluminum profiles that are used in most of the production line. This allows the base structure to easily adapt and be fixed in every part of the main structure of the conveyors that uses Rexroth aluminum profiles. This can be performed resorting to the same Rexroth brackets that are used in the connections of the aluminum profiles within the overflow cure system itself.

6. Conclusions and future work

In a general way, most of what was studied or developed in this project provided new information about the process and its characteristics, being that it can either be considered for the specific application that this project was designed for or a *lesson learned* for future work.

The following points refer the main achievements or conclusions that this work provided within the many domains involved in its development, given that the first two points correspond to the main goal that motivated it:

- **LOCA overflow can be controlled resorting to local cure of the zones affected by this problem through hot air convection;**
- **The final version of the OCS, system designed to cure overflow by applying a hot air stream locally, is able to perform this function and can be adapted to install in line providing an automatized solution, hence eliminating the number of rejections relative to the problem of overflow of LOCA;**
- The OCS has a steady response within a range of ± 3 °C in turn of the reference temperature, so the accuracy of the system should be improved integrating a PID controller in the system;
- The time of exposure of the product to this early cure process is more significant than the temperature for the objective of achieving cure of the LOCA that flows out of the active area of the display;
- The best results occurred with the parameterization of 9 minutes with 95 °C, with 95% of confidence for the factor Time and 90% of confidence for the factor Temperature;
- In regards to future work the system should be tested with improved accuracy for a stage of 9 minutes, but within a bigger range of temperatures. The maximum temperature tested should be kept at the maximum operating temperature of the

product, but the minimum should be 65 °C which may lead to cure the material within 9 minutes according to Table 1;

- Also in the field of future work, different nozzles should be tried, to access if the air flow may be optimized to start the cure reaction in this zones faster;
- The air curtains, which are considerably big aluminum components in contact with the hot air stream proved to be a poor choice to dispense the air, since they are the most dissipative elements in the first version of the system. Also these components are not suitable to be isolated since a great part of the external surface is used to guide the air;

References

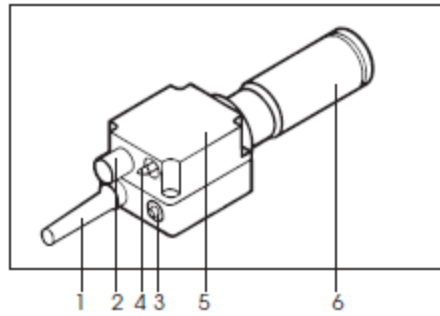
- [1] D. Bonn, Eggers, Jens, Joseph Indekeu, Meunier, Jacques and Rolley, Etienne, "Wetting and spreading," *Reviews of modern physics*, vol. 81, 2009.
- [2] Planar. *Optical Bonding*.
- [3] B. Bahadur, J. D. Sampica, J. L. Tchou, and A. Butterfield, "Direct dry film optical bonding-A low-cost, robust, and scalable display lamination technology," *Journal of the Society for Information Display*, vol. 19, no. 11, pp. 732-740, 2011.
- [4] EIZO. http://www.eizoglobal.com/library/basics/eizo_optical_bonding/index.html.
- [5] M. T. J. A. B. E. S. E. D. N. M. A. N. A. M. M. J. C. M. S. A. F. M. C. S. M. F. M. M. P. Y. KOK "Method for bonding two layers with liquid adhesive and bonded assembly thereof," 2015.
- [6] G. Digital. <http://www.generaldigital.com/optical-bonding-of-flat-panel-displays>.
- [7] J. D. S. Birendra Bahadur, Joseph L. Tchou, and Vince P. Marzen. (2013). *Direct-Dry-Film Optical Bonding: Finding New Applications*.
- [8] D. a. Franck, "Wall phenomena in a critical binary mixture," *Phys. Rev. Lett.*, vol. 59, no. 555, 1987.
- [9] J. B. Brzoska, N. Shahidzadeh, and F. Rondelez, "Evidence of a transition-temperature for the optimum deposition of grafted monolayer coatings," *Nature (London)*, vol. 360, no. 719, 1992.
- [10] S. Wu, "Modifications of polymer surfaces: Mechanisms of wettability and bondability improvements," *Polymer Interfaces and Adhesion (Dekker, New York)*, pp. 279-329, 1982.
- [11] Krüss.de.
- [12] T. Young, "An essay on the cohesion of fluids," *Philos. Trans. R. Soc. London*, vol. 95, no. 65, 1805.
- [13] D. Bonn, E. Bertrand, N. Shahidzadeh, K Ragil, H. T. Dobbs, A. I. Posazhennikova, D. Broseta, J. Meunier, and J. O. Indekeu, 2001, "Complex wetting phenomena in liquid mixtures: Frustrated-complete wetting and competing intermolecular forces,," *J. Phys.: Condens. Matter*, vol. 13, no. 4903, 2001.
- [14] F. Brochard-Wyart, J. M. de Gennes, D. Quéré, and P.-G. de Gennes, "Spreading of nonvolatile liquids in a continuum picture," *Langmuir*, vol. 7, no. 335, 1991.
- [15] P.-G. de Gennes, F. Brochart-Wyart, and D. Quéré, "Capillarity and Wetting Phenomena: Drops, Bubbles, Pearls, Waves," *Springer, New York*, 2003.

- [16] R. Seemann, S. Herminghaus, and K. Jacobs, "Gaining control of pattern formation of dewetting liquid films," *Phys.: Condens.*, vol. 4925, no. 13, 2001b.
- [17] R. Seemann, S. Herminghaus, C. Neto, S. Schlagowski, D. and R. K. Podzimek, H. Mantz, and K. Jacobs, "Dynamics and structure formation in thin polymer melt films,," *J. Phys.: Condens. Matter*, vol. S267, no. 17, 2005.
- [18] G. McHale, "Dewetting — the opposite of spreading," ed: Northumbria University, 2016.
- [19] V. S. Mitlin, "Dewetting of solid surface: analogy with spinodal decomposition," *J. Colloid Interface Sci.*, vol. 491, no. 156, 1993.
- [20] D. C. Montgomery, *Introduction to Statistical Quality Control*, 6th ed.
- [21] *Meet Minitab 15*. 2007.
- [22] *Meet Minitab 18*. 2017.
- [23] P.-G. De Gennes, F. Brochard-Wyart, and D. Quéré, "Capillarity and Gravity," in *Capillarity and Wetting Phenomena*: Springer, 2004, pp. 33-67.
- [24] R. Anitha, S. Arunachalam, and P. Radhakrishnan, "Critical parameters influencing the quality of prototypes in fused deposition modelling," *Journal of Materials Processing Technology*, vol. 118, no. 1, pp. 385-388, 2001/12/03/ 2001.
- [25] R. F. Steve Upcraft, "The rapid prototyping technologies", *Assembly Automation*, vol. 23, no. 4, pp. 318-330, 2003.

A. Attachment of Technical sheets

This section shows the attachments of the technical sheets of standard components and drawings of customized components.

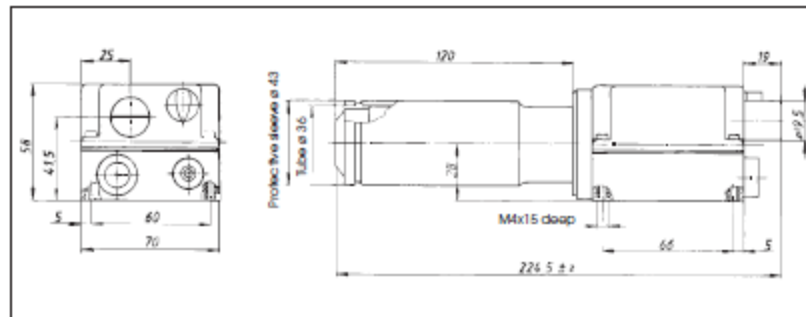
Description of tool



1. Protective sleeve for cable to mains
2. Air intake connection Ø 19.5
3. Potentiometer for temperature adjustment
4. Air regulating knob
5. Connection housing
6. Element housing with protective sleeve

Installation

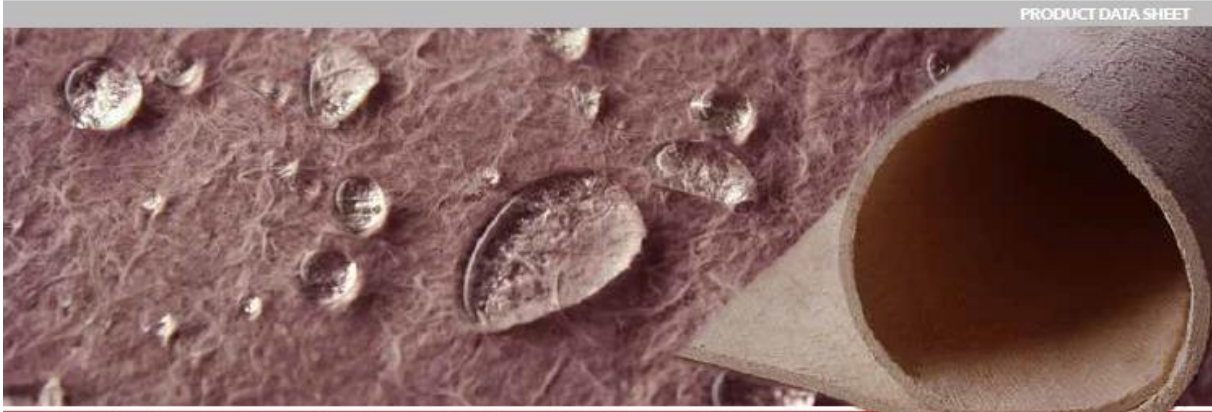
- The tool should be fixed by using four M4 screws on the **connection housing (5)**.
- When installing the tool, ensure that:
 - only cold air is sucked in
 - no (warm air) back pressure develops
 - the hot air tool is not in direct line of another hot air tool.
- Protect the tool from vibration and shock.
- Installation dimensions in mm



Air supply

- LEISTER blowers must be used for the air supply (pay attention to the direction of rotation and the electrical connection).
- For use in a dusty environment the tool should be fitted with a LEISTER stainless steel filter on the air intake connection. Where a particularly critical dust problem exists (eg metal, electrically charged or damp dust) special filters must be used to avoid short circuiting the tool.
- The hot air tool should only be supplied with air up to a max. 50°C.
- The minimum air flow must be observed (see page 2).

TECHNICAL DATA			
Voltage	V-	220-230	120
Frequency	Hz	50 / 60	
Capacity	W	3000	2200
Minimum air flow	l/min	300	200
Maximum temperature	°C	650	650
Ambient temperature	°C	<60	<60
Weight	kg	0,5	0,5
Size	mm	227 x 70 x 58	



PRODUCT DATA SHEET

High-Performance Aerogel Insulation for Industrial and Commercial Applications

Pyrogel® XTE is a flexible, high-performance, aerogel blanket insulation designed for use in industrial and commercial applications. Pyrogel XTE is engineered to deliver superior thermal performance while offering excellent protection against corrosion under insulation (CUI). Hydrophobic and breathable, Pyrogel XTE ensures long-lasting water resistance for both the insulation layer and underlying asset; they remain drier for longer, preserving process conditions, and saving energy in the harshest of environments. These characteristics make Pyrogel XTE the “go-to” insulation for industry-leading CUI defense.

With its extremely low thermal conductivity, Pyrogel XTE is up to 75% thinner than competing materials. Its thin profile makes it ideal for installation in congested areas or to resolve mechanical clashes, increasing both plant safety and efficiency. Pyrogel XTE is mechanically robust, enabling pre-insulation to save time and money. It can be removed and reused after inspection, lowering total cost of ownership.

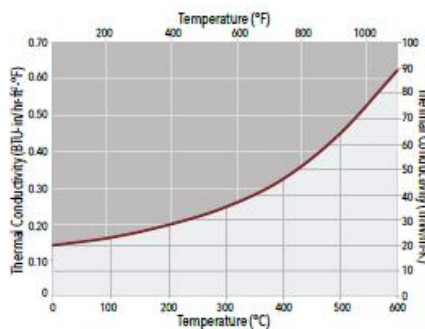
The versatility of Pyrogel XTE makes it suitable for a wide range of applications, from small-bore pipe to the largest format process vessels and equipment.

THERMAL CONDUCTIVITY†

† Tested in accordance with ASTM C177

Mean Temp. °F / °C	k BTU-in/hr-ft ² -°F / mW/m-K
32 / 0	0.14 / 20
212 / 100	0.16 / 23
392 / 200	0.19 / 28
572 / 300	0.24 / 35
752 / 400	0.32 / 46
932 / 500	0.44 / 64
1112 / 600	0.62 / 89

† Thermal conductivity measured at a compressive load of 2 psi.



ADVANTAGES

- Best-in-class CUI protection
- Hydrophobic and breathable, resists liquid water and avoids the damaging effects of wet insulation
- Up to five-times better thermal performance versus competing materials
- Faster application rates, especially on large-bore pipes and vessels
- Tough enough to maintain thermal performance even after compression events
- Versatile format can be cut to fit any piece of piping or equipment
- Reduced logistics costs relative to rigid insulation—lower scrap, transport costs, and man hours on project and turnaround work
- Durable format permits pre-insulation and reuse

Data sheet
Superwool® blanket

Metric information

Contact

Europe:
Telephone:
+44 (0) 151 334 4030

E-mail:
marketing.zo@morganplc.com

North America:
Telephone:
+1 (706) 796 4200

E-mail:
northamerica.zo@morganplc.com

South America:
Telephone:
+54 (11) 4373 4439

E-mail:
marketing.zo@morganplc.com

Asia:
Telephone:
+65 6595 0000

E-mail:
asia.mo@morganplc.com

	Superwool Plus blanket					Superwool HT blanket				
	1200					1300				
Classification temperature, °C	White					White				
Colour	White					White				
Density, kg/m³	64	80	96	128	160	64	96	128	160	
Thermal conductivity, ASTM C-201, W/m K	@200°C	0.06	0.06	0.05	0.05	0.04	-	0.05	0.04	-
	@400°C	0.11	0.09	0.09	0.08	0.07	-	0.10	0.08	-
	@600°C	0.18	0.15	0.14	0.12	0.11	-	0.19	0.14	-
	@800°C	0.29	0.24	0.21	0.18	0.16	-	0.32	0.23	-
	@1000°C	0.42	0.36	0.29	0.25	0.23	-	0.48	0.34	-
	@1200°C	-	-	-	-	-	-	0.69	0.48	-
Tensile strength, EN 1094-1, kPa	30	45	55	75	90	30	50	75	95	
Permanent linear shrinkage, EN 1094-1, % after 24 hours isothermal heating, %	@1200°C					-				
	-					-				
Chemical composition, %	SiO ₂					70 - 80				
	CaO+MgO					18 - 25				
	CaO					-				
	MgO					-				
	Other oxides					<3				

Availability and Packaging

Superwool® HT Blanket are packed in cartons, 1260 x 940mm pallet + stretchable film. Marks (o) and width 1220mm upon request (subject to minimum order requirements).

Superwool® Plus blanket

Thickness mm	Density kg/m³					Length mm	Width mm	Carton m³
	64	80	96	128	160			
6	-	-	-	-	-	4 x 3500	610	13.42
10	-	-	-	-	-	1850	610	11.28
13	-	-	-	-	-	14640	610	8.93
19	-	-	-	-	-	9760	610	5.95
25	-	-	-	-	-	7320	610	4.46
38	-	-	-	-	-	4880	610	2.98
50	-	-	-	-	-	3660	610	2.23

Superwool® HT blanket

Thickness mm	Density kg/m³				Length mm	Width mm	Carton m³
	64	96	128	160			
6	-	-	-	-	4 x 3500	610	13.42
10	-	-	-	-	1850	610	11.28
13	-	-	-	-	14640	610	8.93
19	-	-	-	-	9760	610	5.95
25	-	-	-	-	7320	610	4.46
38	-	-	-	-	4880	610	2.98
50	-	-	-	-	3660	610	2.23

While the values and application information in this database are typical, they are given for guidance only. The values and the information given are subject to normal manufacturing variation and may be subject to change without notice. Morgan Advanced Materials - Thermal Ceramics makes no guarantee and gives no warranty about the suitability of products and you should seek advice on conditions of the product's suitability for use with Morgan Advanced Materials - Thermal Ceramics.

SUPERWOOL® is a patented technology for high temperature insulation wools which have been developed to have a low Uo permeation (informal on upon request). SUPERWOOL® products may be covered by one or more of the following patents, or their foreign equivalents:
SUPERWOOL® PLUS and SUPERWOOL® HT products are covered by patent numbers: US714421 and US7430641, US3,519,645, US7875546, EP1564137 and EP172803 repeatedly.

All other foreign patent numbers is available upon request to Morgan Advanced Materials plc.

Morgan Advanced Materials plc Registered in England & Wales at Quadrant, St-57 High Street, Windsor, Berkshire SL4 1LP, UK. Company No. 281772

Attachment A-3 - Technical sheet of Superwool Blanket from Morgan Ceramics


Superwool®

Superwool® Plus Blanket



Main properties

Classification temperature	1200°C
Maximum continuous use temperature	1000°C
Colour:	White
Density:	64, 80, 96, 128, 160 kg/m ³ (4, 5, 6, 8, 10) lbs/ft ³
Tensile strength:	128 kg/m ³ 75 kPa

High Temperature Performance

Permanent linear shrinkage after 24 hours isotherm heating at 1200°C: 1%

Thermal Conductivity (ASTM C-201)

Following the decision by the European standards committee to withdraw the Thermal Conductivity test according to EN 1094-1 as being inaccurate, Morgan Thermal Ceramics has decided to quote all Thermal Conductivity data according to the well established ASTM C-201 method.

		Thermal conductivity (ASTM C-201):			
Mean Temperature	W/mK (BTU.in/hr/ft ² °F)	64 kg/m ³ 4 lbs/ft ³	80 kg/m ³ 5 lbs/ft ³	96 kg/m ³ 6 lbs/ft ³	128 kg/m ³ 8 lbs/ft ³
200°C	392 °F	0.06 (0.42)	0,06 (0,42)	0,05 (0,35)	0,05 (0,33)
400°C	752 °F	0.11 (0.76)	0,09 (0,62)	0,09 (0,62)	0,08 (0,55)
600°C	1112 °F	0.18 (1.24)	0,15 (1,04)	0,14 (0,97)	0,12 (0,83)
800°C	1472 °F	0.29 (2.00)	0,24 (1,66)	0,21 (1,46)	0,18 (1,25)
1000°C	1832 °F	0.42 (2.9)	0,36 (2,49)	0,29 (2,01)	0,25 (1,73)

Chemical Composition

SiO₂: 62-68%
CaO: 26-32%
MgO: 3-7%
Other: <1%

Availability & Packaging

Superwool® Plus Blankets are packed in cartons, 1280 x 940mm pallet + stretchable film.
Contact your local Morgan Thermal Ceramics sales office for advice on availability.

Thickness mm	64 kg/m ³	80 kg/m ³	96 kg/m ³	128 kg/m ³	160 kg/m ³	Length mm	Width mm	m ² /carton
6				X		4 x 5500	610	13.42
10			X	X		18500	610	11.28
13		X	X	X	X	14640	610	8.93
19	X	X	X	X	X	9760	610	5.95
25	X	X	X	X	X	7320	610	4.48
38	X	X	X	X		4880	610	2.98
50	X	X	X	X		3660	610	2.23

Densities marked * and width of 1220mm are available upon request (subject to minimum order requirements).

The values given herein are typical values obtained in accordance with accepted test methods and are subject to normal manufacturing variations. They are supplied as a technical service and are subject to change without notice. Therefore, the data contained herein should not be used for specification purposes. Check with your Thermal Ceramics office to obtain current information.

Attachment A-4 - Technical sheet of Superwool Plus Blanket from Morgan Ceramics

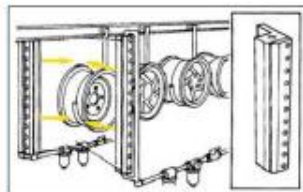


Energy Saving Air Curtain

The Air Curtain from Meech Air Technology provides an efficient blade of air for wide area blow-off and drying applications. When used to replace drilled or slotted lengths of pipe, which consume vast volumes of compressed air, the Air Curtain offers compressed air savings of up to 70%.

APPLICATIONS:

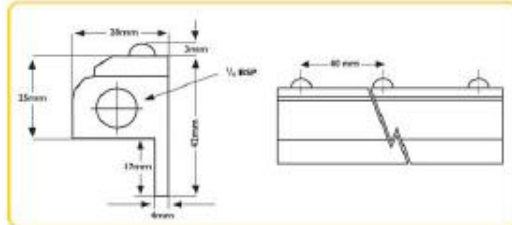
- Product drying
- Product cooling
- Swarf contamination removal
- Air saving: reduction of energy bills
- Compressor demand reduction
- Noise reduction



Powder Coating and Curing

Two Model A85024 600mm Air Curtains cool wheel rims as they exit powder coating ovens.

DIMENSIONS:



How it works:

The Air Curtain releases a small volume of compressed air through a .002" (.508mm) slot along its entire length. The 'blade' of air travels down the front face of the Air Curtain creating an area of low pressure behind it that entrains ambient air at a ratio of up to 25:1, delivering a massive airflow to the target.

FEATURES AND BENEFITS:

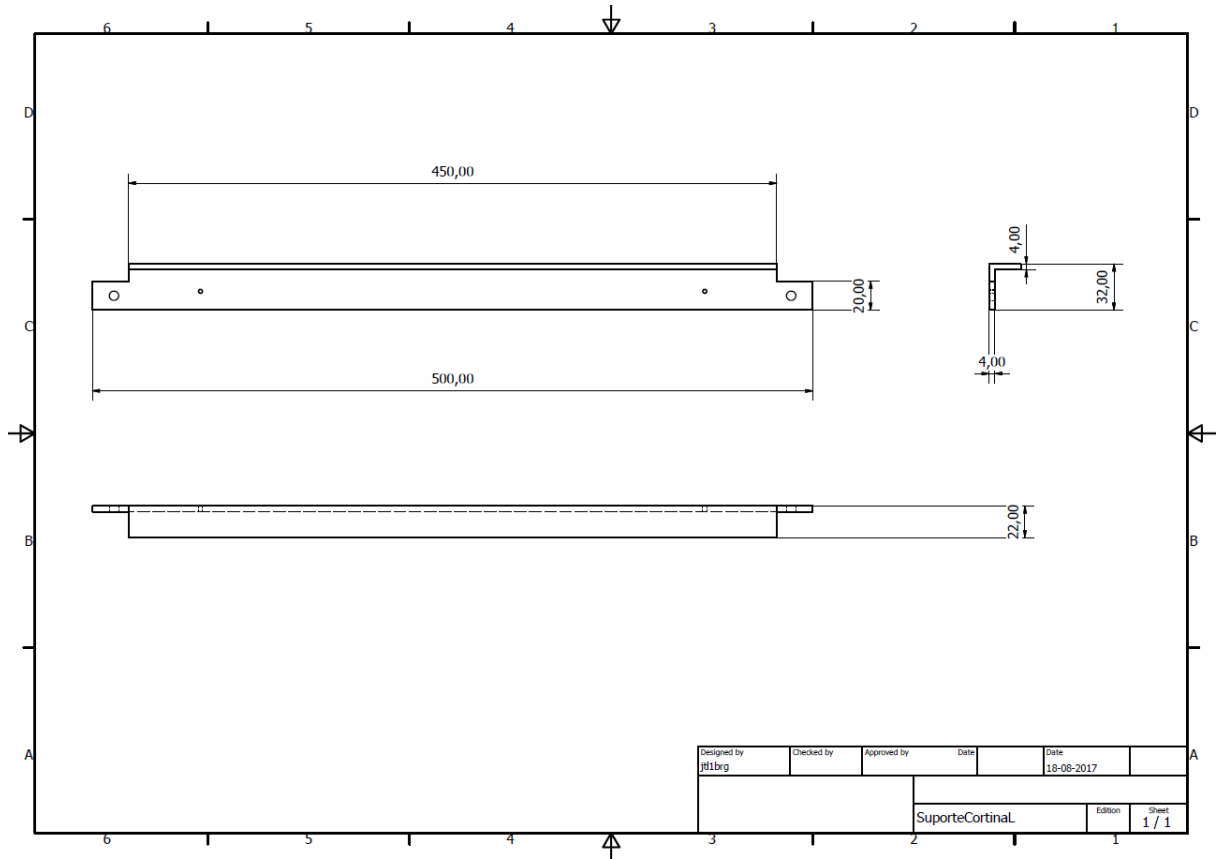
- | | |
|--|--|
| <p>Innovative design</p> <p>No moving parts</p> <p>Adjustability</p> <p>Flange</p> | <ul style="list-style-type: none"> - 25:1 air amplification - Up to 50dBA noise reduction - Health and Safety compliant - Low maintenance - Application specific set-up - Ease of mounting |
|--|--|

PRODUCT NUMBERS AND DESCRIPTIONS:

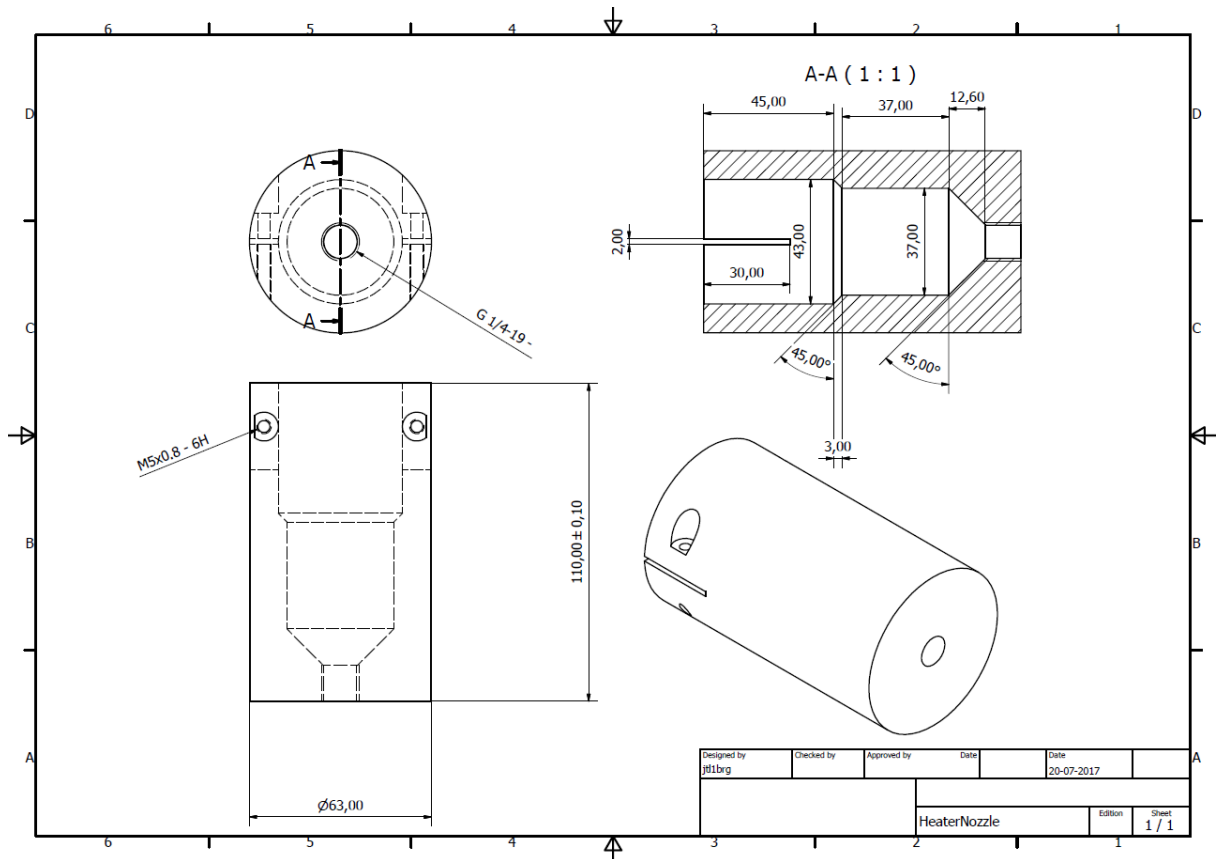
Aluminium		Aluminium			
A85003	-	80mm Air Curtain	A85030	-	750mm Air Curtain
A85006	-	150mm Air Curtain	A85036	-	900mm Air Curtain
A85012	-	300mm Air Curtain	A85048	-	1200mm Air Curtain
A85018	-	450mm Air Curtain	A85055	-	1400mm Air Curtain
A85024	-	600mm Air Curtain	A85071	-	1800mm Air Curtain

Any length between 50mm and 2000mm can be manufactured to order. Hard Anodised and Stainless Steel units are available on request.

Attachment A-5 - Technical sheet of Air Curtain from Meech Air Technology



Attachment A-6 - Technical drawing of custom support for Air Curtains



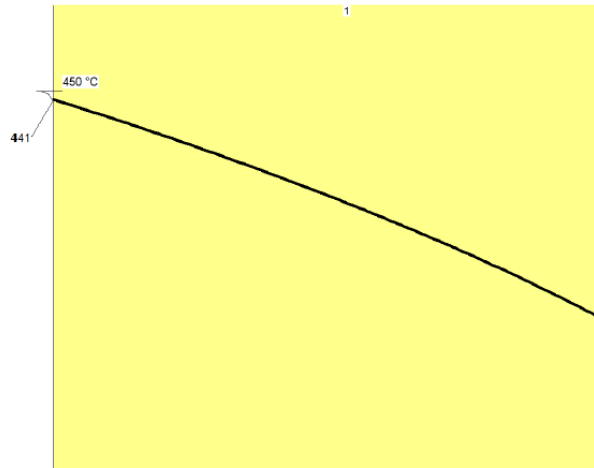
Attachment A-7 Technical drawing of custom heater nozzle

Control of LOCA overflow in Optical Bonding process

	inside	outside	unit	lining characteristics
Ambient temperature	450	20	°C	1299 W/m2 heat loss
Surface temperature	441.3	191.7	°C	0.4978 MJ/m2 heat storage
Heat transition coefficient	150	7.564 ⁽¹⁾	W/m2K	1.664 kg/m2 weight
				13 mm total thickness

(1) Calculated with ASTM C680, issue 2004 Emissivity=0.05 - wind=0 m/s

<u>wall layers from inside to outside</u>				temperature		
Material	Thickn. mm	Density kg/m3	Classif. °C	border °C	mean °C	K mean W/mK
1 Superwool 607 Plus-128	13	128	1140	441.3	328	0.0692
				191.7		

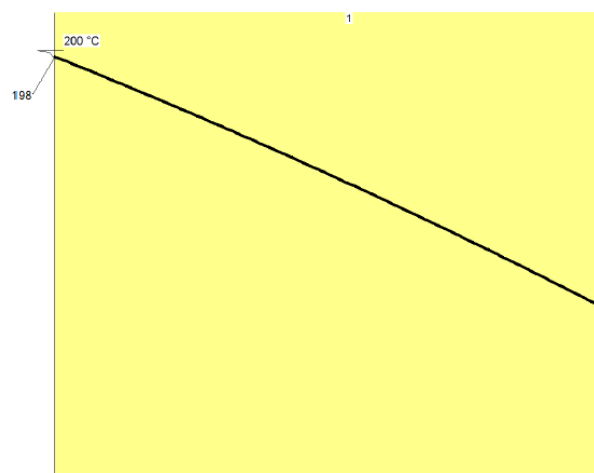


Attachment A-8 - First half of temperature profile on Superwool coating 128 kg/m³ with 13 mm thickness

	inside	outside	unit	lining characteristics
Ambient temperature	200	20	°C	373.1 W/m2 heat loss
Surface temperature	197.5	85.3	°C	0.1792 MJ/m2 heat storage
Heat transition coefficient	150	5.715 ⁽¹⁾	W/m2K	1.664 kg/m2 weight
				13 mm total thickness

(1) Calculated with ASTM C680, issue 2004 Emissivity=0.05 - wind=0 m/s

<u>wall layers from inside to outside</u>				temperature		
Material	Thickn. mm	Density kg/m3	Classif. °C	border °C	mean °C	K mean W/mK
1 Superwool 607 Plus-128	13	128	1140	197.5	144	0.0431
				85.3		



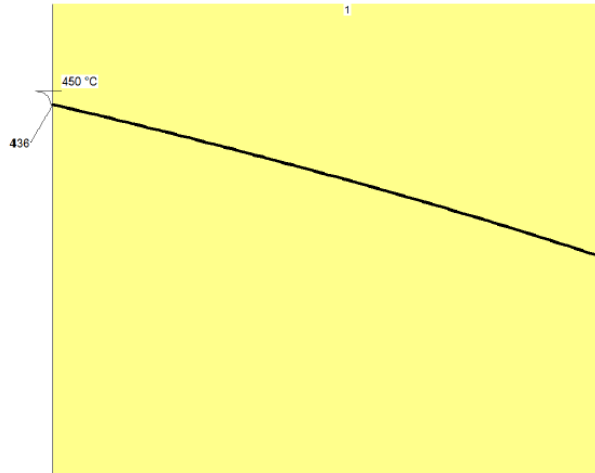
Attachment A-9 - Second half of temperature profile on Superwool coating 128 kg/m³ with 13 mm thickness

Control of LOCA overflow in Optical Bonding process

	inside	outside	unit	lining characteristics
Ambient temperature	450	20	°C	2070 W/m ² heat loss
Surface temperature	436.2	265.7	°C	0.2531 MJ/m ² heat storage
Heat transition coefficient	150	8.423 ⁽¹⁾	W/m ² K	0.768 kg/m ² weight
				6.0 mm total thickness

(1) Calculated with ASTM C680, Issue 2004 Emissivity=0.05 - wind=0 m/s

wall layers from inside to outside				temperature		
Material	Thickn. mm	Density kg/m ³	Classif. °C	border °C	mean °C	K mean W/mK
1 Superwool 607 Plus-128	6.0	128	1140	436.2	356	0.0734
				265.7		

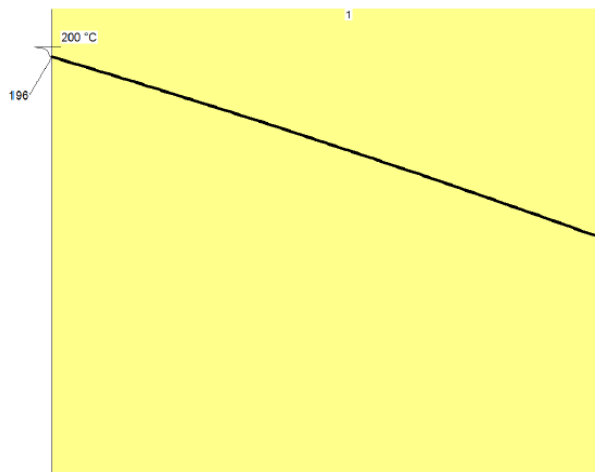


Attachment A-10 - First half of temperature profile on Superwool coating 128 kg/m³ with 6 mm thickness

	inside	outside	unit	lining characteristics
Ambient temperature	200	20	°C	603.1 W/m ² heat loss
Surface temperature	196.0	114.7	°C	0.0923 MJ/m ² heat storage
Heat transition coefficient	150	6.369 ⁽¹⁾	W/m ² K	0.768 kg/m ² weight
				6.0 mm total thickness

(1) Calculated with ASTM C680, Issue 2004 Emissivity=0.05 - wind=0 m/s

wall layers from inside to outside				temperature		
Material	Thickn. mm	Density kg/m ³	Classif. °C	border °C	mean °C	K mean W/mK
1 Superwool 607 Plus-128	6.0	128	1140	196	157	0.0445
				114.7		



Attachment A-11- Second half of temperature profile on Superwool coating 128 kg/m³ with 6 mm thickness

Key Parameter	Description	Unit
Screen size (diagonal)	6.5	inch
Aspect ratio	16.3:9	-
Display resolution	800RGBx480	-
Pixel configuration	RGB – stripe 0.05975(x3) x 0.16525	mm ²
LCD technology	Active matrix TFT	-
Image mode	Normally black	-
Display type	Transmissive	-
Brightness	950	Cd/m ²
Backlight	12pcs LED	
Display Colors	262K(6 bits) / 16.2M (8 bits)	
Module type	Micro Module: Panel+ICs, LED Backlight and FPC	-
Operating Temperature	-30 to +85 (Panel surface temperature)	°C
Storage Temperature	-40 to +95 (Ambient temperature)	°C
Electronics and interface		
Panel interface	RSDS	
Mechanical dimensions		
Width	157.9	mm
Height	94.37	mm
Thickness	6.44	mm
Active area dimensions Width x Height	143.4 x 79.32	mm ²
Basic display features		
Preferred viewing direction	Horizontal axis	-
Surface treatment	AG	-
Visibility with polarised sunglass	Readable	-

Attachment A-12 – General specifications from product specification of the display

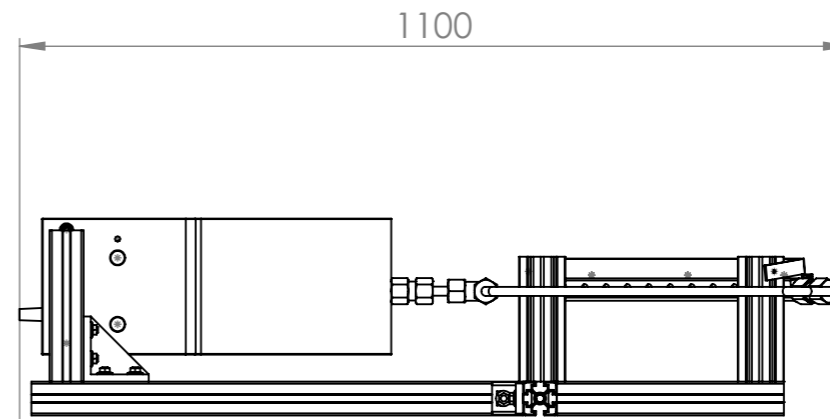
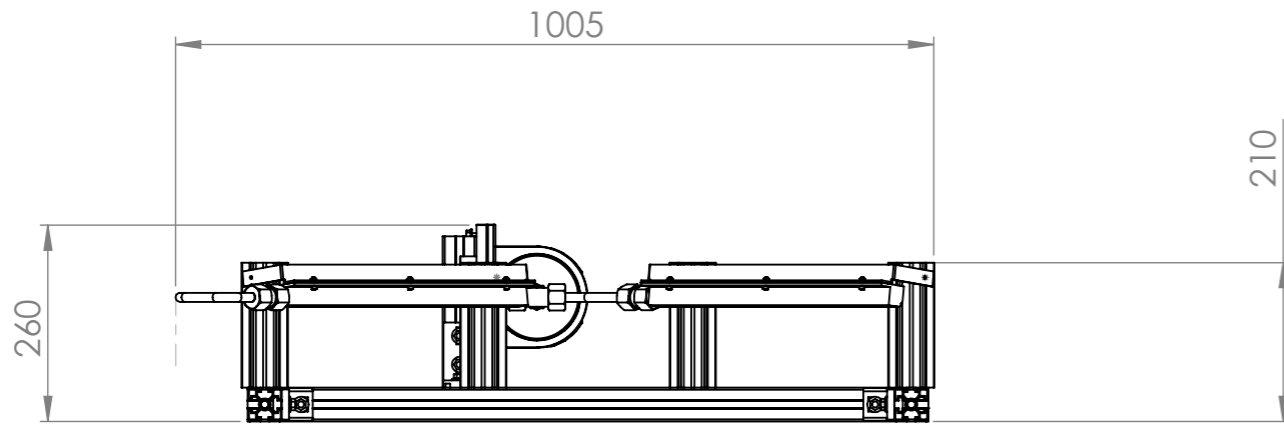
B. Attachment of Technical Drawings of OCS

In this chapter one can observe the technical drawing and the exploded view of the first version of the OCS that is presented in chapter 4.

8 7 6 5 4 3 2 1

F

F

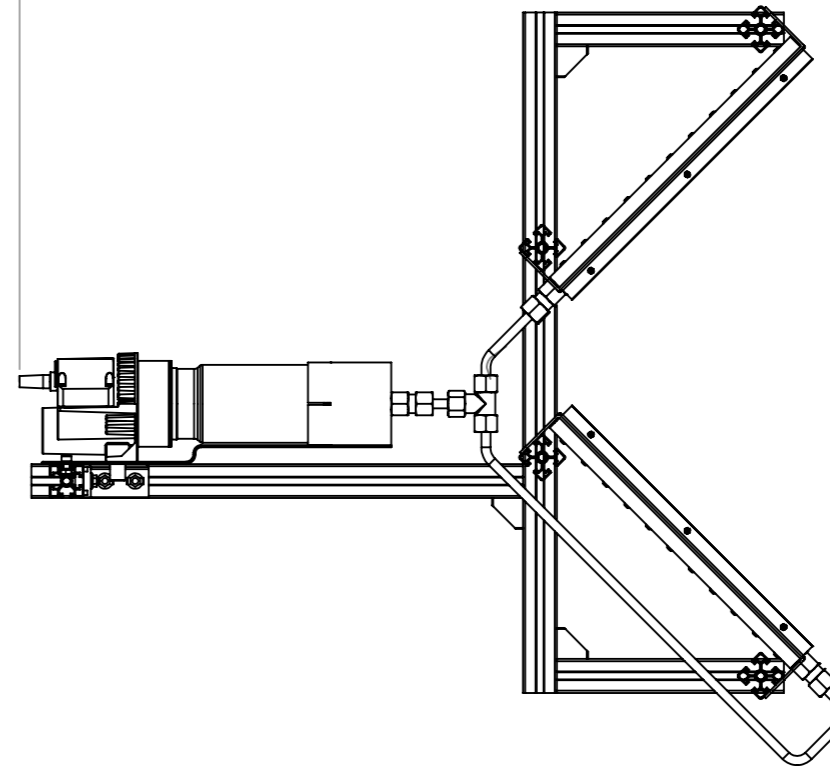
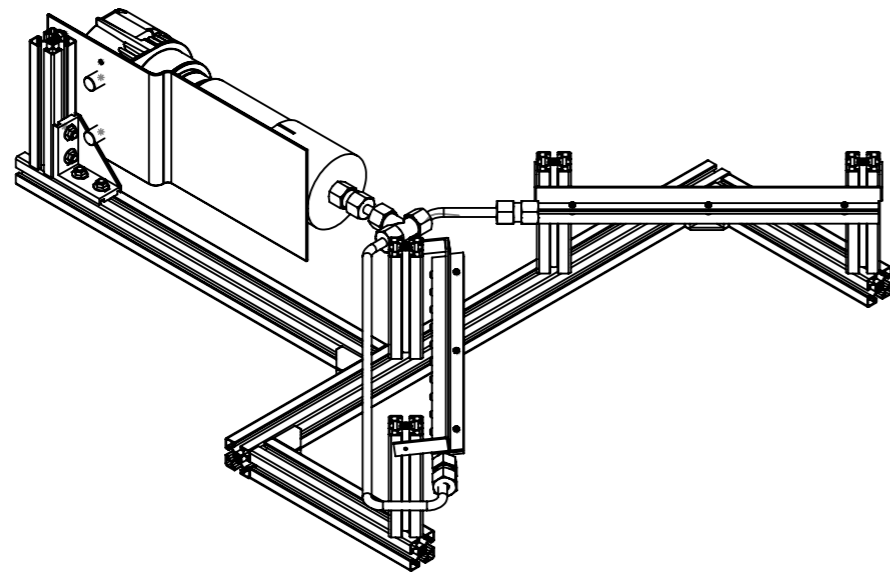


E

E

D

D



C

C

B

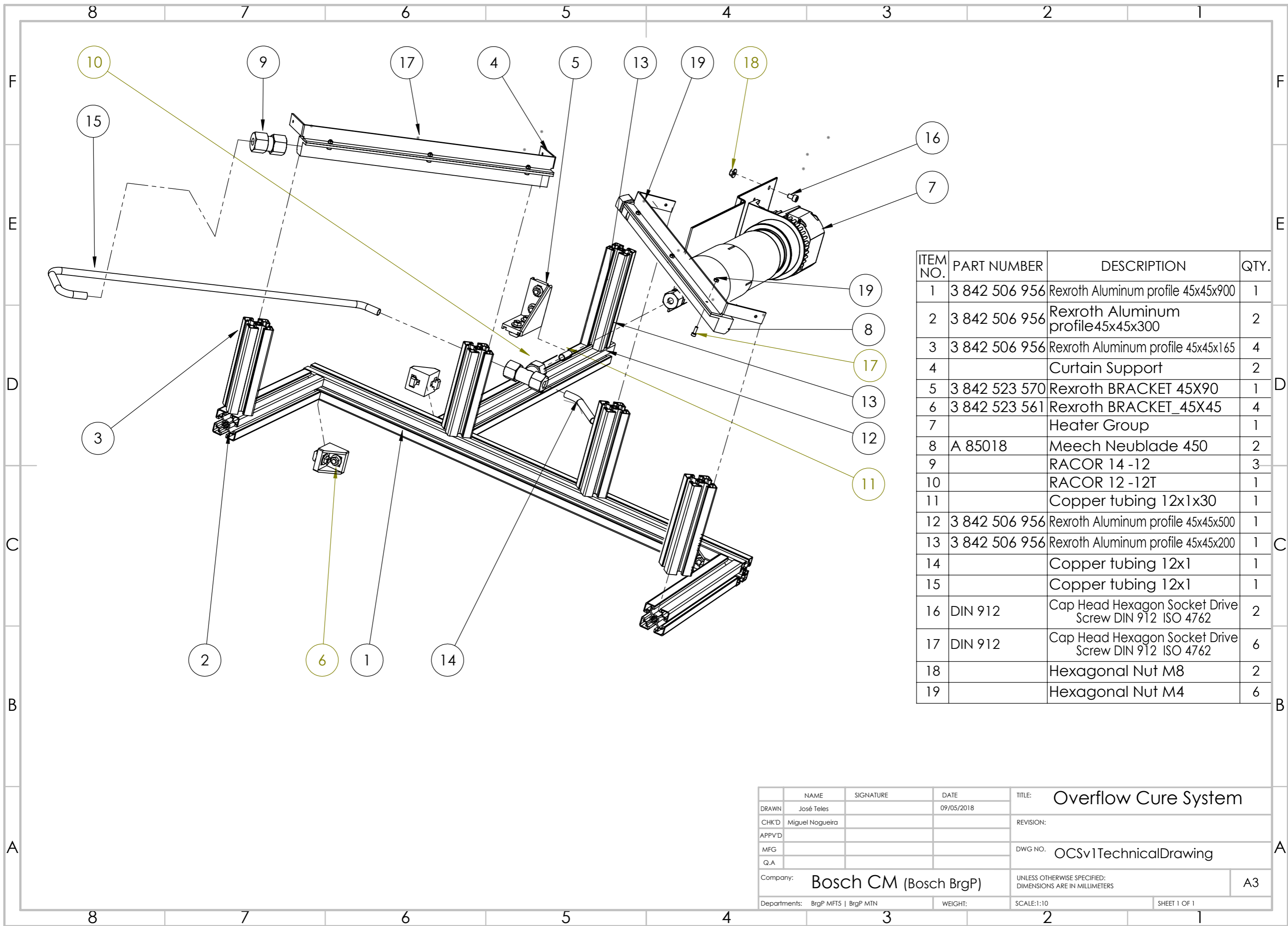
B

A

A

8 7 6 5 4 3 2 1

	NAME	SIGNATURE	DATE	TITLE: Overflow Cure System
DRAWN	José Teles		09/05/2018	REVISION:
CHK'D	Miguel Nogueira			DWG NO. OCSv1TechnicalDrawing
APPV'D				
MFG				
Q.A				
Company: Bosch CM (Bosch BrgP)			UNLESS OTHERWISE SPECIFIED: DIMENSIONS ARE IN MILLIMETERS	
Departments: BrgP MFTS BrgP MTN			WEIGHT:	A3
			SCALE:1:20	SHEET 1 OF 1



ITEM NO.	PART NUMBER	DESCRIPTION	QTY.
1	3 842 506 956	Rexroth Aluminum profile 45x45x900	1
2	3 842 506 956	Rexroth Aluminum profile 45x45x300	2
3	3 842 506 956	Rexroth Aluminum profile 45x45x165	4
4		Curtain Support	2
5	3 842 523 570	Rexroth BRACKET 45X90	1
6	3 842 523 561	Rexroth BRACKET_45X45	4
7		Heater Group	1
8	A 85018	Meech Neublade 450	2
9		RACOR 14 -12	3
10		RACOR 12 -12T	1
11		Copper tubing 12x1x30	1
12	3 842 506 956	Rexroth Aluminum profile 45x45x500	1
13	3 842 506 956	Rexroth Aluminum profile 45x45x200	1
14		Copper tubing 12x1	1
15		Copper tubing 12x1	1
16	DIN 912	Cap Head Hexagon Socket Drive Screw DIN 912 ISO 4762	2
17	DIN 912	Cap Head Hexagon Socket Drive Screw DIN 912 ISO 4762	6
18		Hexagonal Nut M8	2
19		Hexagonal Nut M4	6

NAME	SIGNATURE	DATE	TITLE: Overflow Cure System
DRAWN José Teles		09/05/2018	REVISION:
CHK'D Miguel Nogueira			DWG NO. OCSv1TechnicalDrawing
APPV'D			UNLESS OTHERWISE SPECIFIED: DIMENSIONS ARE IN MILLIMETERS
MFG			
Q.A			A3
Company: Bosch CM (Bosch BrgP)		WEIGHT:	SCALE:1:10
Departments: BrgP MFTS BrgP MTN			SHEET 1 OF 1